


ORIGINAL ARTICLE

Effects of pairing on color change and central gene expression in lined seahorses

Sabrina L. Mederos¹ | Rafael C. Duarte² | Mira Mastoras³ | Megan Y. Dennis³ |
 Matthew L. Settles⁴ | Allison R. Lau^{1,5} | Alexandria Scott⁵ | Kacie Woodward⁶ |
 Colby Johnson⁷ | Adele M. H. Seelke^{8,9} | Karen L. Bales^{5,8,9} 

¹Animal Behavior Graduate Group, University of California, Davis, California, USA

²Centro de Ciências Naturais e Humanas, Universidade Federal do ABC (UFABC), Santo André, Brazil

³Genome Center, MIND Institute, and Department of Biochemistry and Molecular Medicine, University of California, Davis, California, USA

⁴Bioinformatics Core Facility, University of California, Davis, California, USA

⁵California National Primate Research Center, University of California, Davis, California, USA

⁶Campus Veterinary Services, University of California, Davis, California, USA

⁷Evergreen Aquatics, La Center, Washington, USA

⁸Department of Neurobiology, Physiology, and Behavior, University of California, Davis, California, USA

⁹Department of Psychology, University of California, Davis, California, USA

Correspondence

Karen L. Bales, Department of Neurobiology, Physiology, and Behavior, University of California, Davis, CA, USA.

Email: klbales@ucdavis.edu

Funding information

Good Nature Institute; UC-Davis College of Biological Sciences

Abstract

Social monogamy is a reproductive strategy characterized by pair living and defense of a common territory. Pair bonding, sometimes displayed by monogamous species, is an affective construct that includes preference for a specific partner, distress upon separation, and the ability of the partner to buffer against stress. Many seahorse species show a monogamous social structure in the wild, but their pair bond has not been well studied. We examined the gene expression of lined seahorses (*Hippocampus erectus*) during and after the process of pairing in the laboratory as well as color change (luminance), a potential form of social communication and behavioral synchrony between pair mates. When a seahorse of either sex was interacting with its pair mate, their changes in luminance (“brightness”) were correlated and larger than when interacting with an opposite-sex stranger. At the conclusion of testing, subjects were euthanized, RNA was extracted from whole brains and analyzed via RNA sequencing. Changes in gene expression in paired males versus those that were unpaired included processes governing metabolic activity, hormones and cilia. Perhaps most interesting is the overlap in gene expression change induced by pairing in both male seahorses and male prairie voles, including components of hormone systems regulating reproduction. Because of our limited sample size, we consider our results and interpretations to be preliminary, and prompts for further exploration. Future studies will expand upon these findings and investigate the neuroendocrine and genetic basis of these behaviors.

KEYWORDS

luminance, monogamy, pair bond, partner preference

1 | INTRODUCTION

Social monogamy is a social system characterized by pair living, defense of a common territory, and sometimes includes mate-guarding, biparental care, and coordinated behaviors.^{1–3} While this

Sabrina L. Mederos and Rafael C. Duarte should be considered equal co-first-authors.
 Adele M. H. Seelke and Karen L. Bales should be considered equal senior authors.

This is an open access article under the terms of the [Creative Commons Attribution-NonCommercial](https://creativecommons.org/licenses/by-nc/4.0/) License, which permits use, distribution and reproduction in any medium, provided the original work is properly cited and is not used for commercial purposes.

© 2022 The Authors. Genes, Brain and Behavior published by International Behavioural and Neural Genetics Society and John Wiley & Sons Ltd.

behavioral pattern is exhibited by 3%–9% of mammalian species, it is at least as common in fish species.^{3–6} Pair bonding, primarily displayed in species that have a monogamous social structure, is a type of affective attachment between two adults defined by several characteristics including a preference for their partner over a stranger, stress buffering and separation distress.^{7–9}

Social behaviors across different vertebrate taxa, including those related to pair bonding, are modulated by the nonapeptides arginine vasopressin (AVP) and oxytocin (OT), along with their non-mammalian homologs, arginine vasotocin (AVT), isotocin (IT) and mesotocin (MT).^{10,11} Blockade of IT receptors and AVT receptors in monogamous cichlid fishes was shown to reduce affiliative behaviors during bond formation.¹⁰ Density of AVT-immunoreactive fibers within telencephalic nuclei were predictive of social affiliations and mating systems in the closely related butterflyfish.¹² Furthermore, for butterflyfish, OT receptor pattern in various brain regions has been shown to be predictive of pair bonding vs solitary living.¹³ Overexpression of AVP receptors in the ventral striatum of a species of vole that does not readily form pair bonds (the meadow vole) resulted in individuals forming pair bonds.¹⁴ These data show that centrally circulating AVP/AVT and OT/IT regulate pair-bond formation and that receptor distribution plays a critical role in the expression of various patterns of social behavior between closely related species. One hypothesis is that the variation in sociosexual behavior between closely related species may be because of polymorphic genetic mechanisms that allow for rapid changes in the genetic expression of neural substrates that regulate social behavior.¹⁵

Recent studies have explored on a genomic scale other potential mechanisms that may account for differences between monogamous and non-monogamous social systems in closely related species. One study found that across monogamous vertebrates, gene expression varied consistently when species transitioned to a monogamous mating style, and the authors were able to identify several candidate genes associated with this behavioral shift.¹⁶ Another study found 331 genes that were associated with a monogamous mating system in cichlid lineages, independent of species or sex.¹⁷ Examination of differential gene expression may prove informative about underlying mechanisms that promote monogamy and pair bonding.

Field and genetic studies on closely related seahorse species such as *Hippocampus whitei*,¹⁸ *Hippocampus zosterae*,¹⁹ *Hippocampus angustus*,²⁰ *Hippocampus capensis*,²¹ *Hippocampus subelongatus*²² and *Hippocampus abdominalis*²³ confirm the existence of genetic and social monogamy as a frequent social structure in this group. Although to our knowledge, the social system of lined seahorses (*Hippocampus erectus*) has not been studied in the wild, laboratory behavioral data shows that pair mates recognize their partner, and that this recognition depends on olfactory cues.²⁴ These studies also suggest that at least under some circumstances, preference for the partner may not persist with separation or illness of the partner.²⁵ Despite behavioral evidence of social monogamy in the wild for some species, seahorse pair bonding has received only limited attention in laboratory settings, and rarely with standardized tests comparable to those used in mammals.^{26–28} We therefore regard lined seahorses, which we study

here, as a *putatively* pair bonding species, and seek to investigate the dyadic communication and gene expression changes associated with the initial interactions between newly paired males and females.

Seahorse partner communication may be showed through modalities that are not available in pair-bonding mammals. Some seahorse species change color to match their surroundings (e.g., *H. whitei*,¹⁸ *H. reidi*,²⁹ *H. erectus*,³⁰ *H. denise*³¹), which allows these ambush predators to increase the success of prey capture. Research on the behavior of wild seahorses and similar fishes suggests that coloration may act as an important mechanism of social communication, including perhaps a way to reinforce the pair bond.^{19,32} Observations of seahorse color changes are often described as “brightening” with the change being a lighter color rapidly covering most of the body, and occurring during social interactions but not solely during courtship.¹⁹

The main objective of this study was to quantify and study color change as a form of social communication of potential importance to seahorse relationships, and to identify changes in gene expression that may play a part in the formation of putative seahorse pair bonds. To accomplish those goals, 5 days after initial pairing, we performed a standardized partner preference test (PPT). Unfortunately, we did not have enough subjects to conclusively investigate the preference for the partner via proximity, which would be our gold standard measure. However, as a result of the repeated measures nature of the luminance changes, we were able to examine (1) preference for interaction partners based on luminance changes and (2) coordinated behavior in luminance changes during interactions. Color changes of the seahorses' abdomens during the PPT were analyzed based on the seahorse vision model. At the conclusion of testing, subjects were euthanized, and RNA was extracted from whole brains and analyzed via bulk RNASeq. Finally, brain gene expression changes induced by pairing in seahorses were compared to those from prairie voles, which are a well described mammalian model for the neurobiology of pair bonding.^{33,34}

We predicted that lined seahorses would exhibit greater frequency, more correlated and more intense color changes while in proximity to their partner, than while in proximity to a stranger. We expected to find differences in gene expression between paired and unpaired males that were relevant to social behavior and reproduction. With this information we hope to advance investigation into the relationships between pair mates in lined seahorses, and into the underlying neurobiological mechanisms of pair bonding that may be the same or different from those in other vertebrates.

2 | MATERIALS AND METHODS

2.1 | Subjects

Experiments were performed on 10 adult *H. erectus* seahorses (seven males, three females; Table 1) obtained from Ocean Rider Seahorse Farm (Kailua-Kona, HI). Subjects were housed in the Teaching and Research Animal Care Services facility at UC Davis. All experiments were performed under National Institutes of Health guidelines for the

TABLE 1 Basic morphometric traits of the seahorse subjects

Seahorse ID	Sex	Weight (g)	Head length (cm)	Trunk length (cm)	Tail length (cm)	Standard length (cm)
Pair 1 M	M	8	2.561	4.717	8.348	15.626
Pair 1 F	F	9	3.101	5.214	8.147	16.462
Pair 2 M	M	8	2.666	5.215	8.247	16.128
Pair 2 F	F	7	2.403	4.814	7.49	14.707
Pair 3 M	M	16	3.291	5.314	10.521	19.126
Pair 3 F	F	6	2.593	4.445	7.75	14.788
Unpaired M 1	M	5	2.392	4.224	7.836	14.452
Unpaired M 2	M	19	3.334	6.542	10.662	20.538
Unpaired M 3	M	8	2.58	4.886	7.353	14.819
Unpaired M 4	M	11	2.772	5.101	9.204	17.077

care of animals in research and were approved by the Institutional Animal Care and Use Committee of the University of California, Davis.

The seahorse colony was maintained on a 12:12 light: dark cycle with the lights on at 6 AM. The ambient room temperature was maintained at 20–22°C, and water temperature in each tank was maintained at 21–23°C. Artificial seawater was made by combining Instant Ocean Sea Salt (Instant Ocean, Blacksburg, VA) with distilled water to achieve a specific gravity of 1.021–1.026. All tanks contained a substrate of live sand and live rock and were equipped with multiple holdfasts to allow for animal attachment. Tanks were tested 3x a week for ammonia, nitrite, and nitrate levels, and tanks underwent a 50% water change weekly. Seahorses were fed twice daily with thawed frozen mysis shrimp enriched with Vibrance supplement (Ocean Rider, Kailua-Kona, HI).

Male and female seahorses were housed in separate same-sex group housing tanks for 4 months prior to pairing. Unpaired animals remained in these tanks. Tanks used for group housing and behavioral testing were 106 liters (76.2 cm long × 31.75 cm deep × 47 cm tall), and paired subjects were housed in 68.14 liter tanks (50.8 cm long × 26.67 cm deep × 47 cm tall). On the day of pairing, one male and one female seahorse were removed from the group housing tanks and placed together in a 68.14 liter tank. Male and female subjects were allowed to cohabitate for 4–5 days before partner preference testing (Figure S1). At this point, courtship behavior had been observed in all pairs.

2.2 | Partner preference testing

We measured luminance (i.e., brightness) changes in the seahorses during a PPT. In more commonly studied mammalian pair bonded species, breeding pairs show preferential contact and maintain proximity with a familiar partner versus a stranger or opposite-sex conspecific.^{8,33} Formation of this preference is commonly tested in a PPT.³⁵ PPTs have been developed and most widely used in rodent species, although their use in non-rodent monogamous species has grown.^{36–38} The PPT has helped researchers identify many biological and social factors that play a role in pair bonding.³⁶ The setup of the

PPT differs across taxa and across different relevant questions but some factors stay consistent. There is typically a period of cohabitation between the test subject and new partner prior to the test, and then they are both transported to a testing arena, typically divided into three chambers. The middle chamber holds the focal animal and the other two hold the familiar partner and an opposite-sex stranger. The time spent in proximity to the partner versus the stranger is then recorded. Time spent near a particular individual has been found to be a good indicator of preference in some fish species.^{39–41} In this study, we used a modified PPT to examine luminance changes as a potential form of social communication in new seahorse pairs. Because of our small sample size and significant variation in pair behavior, we do not present the preference data here. However, we describe the test as far as it was the social setting in which we quantified color changes.

We conducted the PPT in a 106 liter tank subdivided into three equal sections using custom-made acrylic dividers. The clear dividers allowed the subjects to visually identify each other and included 1 cm diameter perforations to allow for water flow between tank sections. As previously mentioned, work performed by Lin and colleagues²⁴ found that olfactory cues were crucial to mate recognition in female lined seahorses.²⁴ Multiple plastic holdfasts were placed in each section of the testing tank, and adjacent to the acrylic dividers, to allow the seahorses to hitch.

On the day of testing, we removed the focal seahorse from its home tank and placed it in the center section of the testing tank. Its partner seahorse was placed in one adjacent section, and an opposite-sex stranger seahorse was placed in the other adjacent section (See Figure 1). Stranger males were unpaired throughout the duration of the study; stranger females were unpaired for the first (Pair 1) and second (Pair 2) PPT. For the third PPT (Pair 3), the stranger female was part of a different pair and had to be used because all females were paired at that point. Analysis of her color changes, and those of the focal male from Pair 3, do not suggest that the use of a paired female affected results. Partners and strangers were matched by size. The partner side and stranger sides were counter-balanced across tests to avoid a side bias.

A color board was placed to the side of the testing tank to enable analysis of color changes (see below). The subjects were filmed by a Panasonic VX981 camera for 3 h. Behaviors were scored partially

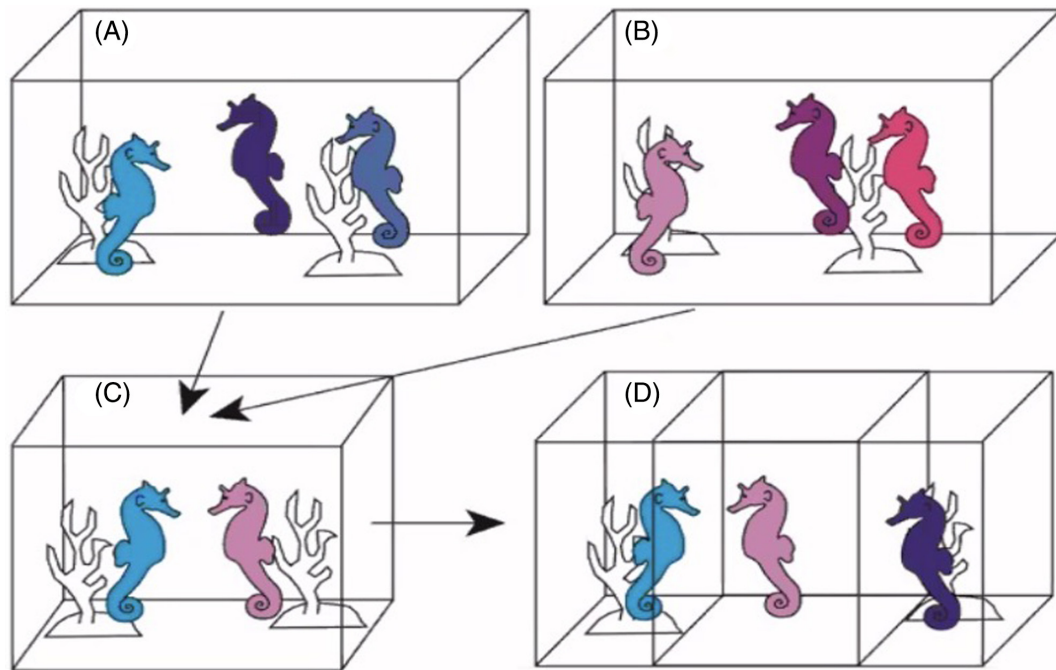


FIGURE 1 We initially housed seahorses in same-sex tanks consisting of all male (A, blue) or all female (B, pink) subjects. At the time of pairing, we placed one male and one female together in a novel tank (C). After 5 days of cohabitation, paired seahorses underwent a partner preference test (PPT) in a large testing tank that was divided into three sections (D). We placed target animals in the center section, partners in one side section, and opposite-sex stranger seahorses in the other side section. Animals interacted for 3 h, during which time their luminance changes were recorded.

blinded (the tanks were labeled, and the animals are sexually dimorphic, but we covered labels during scoring) using BehaviorTracker 1.5 (www.behaviortracker.com). Behaviors scored included the location of the subject and partner/stranger. Within the focal subject section, we further divided the area into three equal zones: proximate to the partner side, proximate to the stranger side, or neutral (in the middle). Proximity was scored when the subject animal was in the relevant zone. Partner and stranger zones were similarly divided. If both the subject and the partner were in the proximity zone at the same time, we scored that as “partner mutual.” If both the subject and the stranger were in the proximity zone at the same time, we scored that as “stranger mutual.” If only the subject was in the proximity zone, in the partner or stranger side, we scored as “partner non-mutual” and “stranger non-mutual,” respectively. These behavioral results were used to determine the location of the seahorse for the analysis of luminance changes.

2.3 | Frame acquisition for seahorse luminance (color) change analysis

We assessed changes in seahorse luminance (i.e., brightness) during the PPT using the six videos (two videos for each of the three pairs). For each video, image frames were extracted at a constant ratio of one frame per second using the software “Free Video to JPG Converter” (<https://www.dvdvideosoft.com/products/dvd/Free-Video-to-JPG-Converter.htm>). Images were saved as JPEG and divided into two

groups of interaction: “mutual interaction,” when the focal seahorse was located within the zone of interaction, close to the respective partner (“partner mutual”) or stranger (“stranger mutual”) individual of the opposite sex; “non-mutual interaction,” when the focal seahorse was located close to the divider wall, but the partner (“partner non-mutual”) or stranger individual (“stranger non-mutual”) was positioned outside the interaction zone. We first counted the frequency of color changes by each sex and type of interaction. We then assessed the baseline luminance of seahorses during periods when individuals were not performing visual color changes. For that, because of the large number of frames, we randomly selected 60 images for each video: 30 for the “partner mutual” and 30 for the “stranger mutual” groups. Visual luminance changes were observed in seahorses for all videos and were characterized by events of rapid (maximum 1 min) changes in the brightness of the seahorse’s abdomen (Figure S2). To quantitatively record those changes under a reliable timeframe, we selected one frame every 4 s for each event of luminance change. In cases where seahorses performed many color alterations, we restricted our analysis to 10 randomly selected events of luminance change because of the large processing time of image analysis.

2.4 | Image analysis and visual modeling

Before obtaining luminance data, each image was linearized ($R^2 \geq 0.999$ for all camera channels) to correct for camera nonlinear pixel responses to light intensity using a color chart (X-rite color

checker).⁴² This procedure was necessary because of the nonlinear response of our video camera to changes in light levels that need to be corrected before obtaining accurate data.⁴³ Images were also equalized for changes in light conditions using 3.2% and 19.2% standards from the color checker and saved as 32-bit multispectral images. All these procedures were performed using functions from the mica Toolbox within the ImageJ software.⁴⁴

Seahorse luminance was analyzed based on a seahorse vision model.^{45,46} Since there is no available information about the visual system of lined seahorses (*H. erectus*), the spectral sensitivities of the closely related species *Hippocampus subelongatus* were used for modeling.⁴⁵ We assumed that the two species would exhibit similar visual capacities since both live in comparable green-water vegetated habitats.^{45,47} The use of visual modeling takes account of the visual system of the appropriate receiver (i.e., the seahorse itself), instead of the human scoring the visual data, which is a much more reliable way to test for the possible functions of color change in the species.

In summary, *H. subelongatus* exhibits single cones absorbing short wavelengths (SWS, spectral peak at 467 nm), and double cones absorbing medium (MWS, spectral peak at 522 nm), medium-long (M-LWS, spectral peak at 537 nm) and long wavelengths (LWS, spectral peak at 560 nm). Since the spectral sensitivity of MWS and M-LWS cones are very similar,⁴⁵ we assumed that one of them is responsible for luminance (i.e., achromatic) contrast, while the other in conjunction with the SWS and LWS cones are responsible for color vision, resulting in a trichromatic visual system. Here, we followed the same protocol used by Duarte and colleagues⁴⁶ and considered the M-LWS cones as responsible for seahorse's luminance vision. We also incorporated to the model a 50% light transmission cut-off at 425 nm⁴⁵ and used a D65 standard irradiance spectrum as a measure of incident illumination,⁴⁸ compatible to the restricted shallow-water environment where visual interactions between seahorses take place. Before building the model, we calculated the spectral sensitivity curves of our video camera using one image frame extracted from a short video of the color chart made under natural illumination,⁴² which allowed us to use a polynomial mapping analysis to convert images from the camera color space into values of seahorse cone catches, closely corresponding to spectrometry techniques.⁴⁴

Visual modeling resulted in multispectral images, which were used to estimate photon catch values for each color channel in the region of interest measured in the seahorse (i.e., the abdominal region of the individual). Whenever possible, we measured in each frame the photon catches of the focal, partner and stranger seahorses during the event of color change. Based on preliminary data, we restrained our analysis to luminance since this was the only channel varying during the events of color change observed in the species. For each luminance change event we calculated the percent luminance change using the following formula:

$$\frac{\text{Maximum luminance} - \text{Minimum luminance}}{\text{Minimum luminance}} * 100.$$

We used descriptive statistics, such as means and standard errors, to represent the baseline luminance of male and female seahorses

during the periods of no color change and used Cohen's d to test variation and trends of baseline luminance between sexes. For luminance change events, we first quantified the number of events performed by seahorses of both sexes during mutual and non-mutual interactions, when the focal seahorse was within the interaction zone of the partner or stranger individual.

We used repeated measures correlation to test whether the luminance change in seahorse pairs during mutual interactions is correlated and whether it is affected by the interaction of the focal seahorse with the partner or the stranger conspecific. We used this method to control for the repeated observations of luminance change made in the same individual of the different pair configurations (i.e., focal x pair and focal x stranger seahorse) we had in video trials. Correlation analyses were conducted through the `rmcorr` function from the "rmcorr"⁴⁹ package in R.

We also examined whether changes in luminance differed between mutual interactions with the focal subject and their partner or an opposite-sex stranger. To do this we identified luminance change events that occurred when the focal animal was in the interaction zone at the same time as their partner (partner mutual interaction) or in the interaction zone at the same time as an opposite-sex stranger (stranger mutual interaction). For each event we calculated the % luminance change for each member of the interaction (i.e., focal subject and partner or focal subject and stranger). The % luminance change was averaged first within subjects then between subjects to get an average % luminance change for each mutual interaction. We did not use non-mutual interactions in both analysis of % luminance change and luminance correlation because of the low number of this type of event in our dataset, which makes it difficult to calculate effect sizes and correlation metrics.

2.5 | Tissue collection and processing

At the conclusion of testing, the subjects were deeply anesthetized through immersion in a bath of 500 mg/kg buffered MS-222 and were euthanized via decapitation. Weight and standard body length measurements (head + trunk + tail length⁵⁰) were taken. All tissue collection occurred between 10 AM and 2 PM. The brain was removed and flash frozen for later RNA extraction. RNA was extracted from whole brains using Qiagen AllPrep DNA/RNA Mini Kit (Qiagen). Whole brains were used because of their small sizes, the low-cellular density of the tissue, and the desire to obtain individual rather than pooled data. The quality and concentration of the extracted RNA was assessed using a NanoDrop spectrophotometer (Thermo Scientific) and an Agilent Bioanalyzer 2100 (Agilent Technologies).

2.6 | RNA sequencing, assembly and annotation

The DNA Technologies and Expression Analysis Core at the Genome Center of the University of California, Davis prepared RNA-Seq libraries from the 10 seahorses and performed sequencing. Barcoded indexed RNA-seq libraries were generated from 1 ug total RNA each after

poly-A enrichment using the Kapa Stranded RNA-seq kit (KapaBiosystems) following manufacturer's instructions. After library preparation, samples were sequenced with Illumina NovaSeq S4 generating 150-bp paired-end (PE) reads.

Bioinformatics analysis was performed at the University of California, Davis Bioinformatics Core Facility. Quality-control and adapter-trimming preprocessing of raw sequence reads were performed using HTStream (<https://github.com/s4hts/HTStream>) to remove technical features such as Illumina adapters, polyAT sequences, PCR duplicates, reads less than 50 bp in length, and low-quality regions below an average quality of 20 from the ends of reads. Once cleaned, reads were aligned to the *Hippocampus comes* genome (assembly: H_comes_QL1_v1) using STAR,⁵¹ and generating a read counts table for each sample and each gene using the corresponding annotation from Ensembl (release 104). Analysis was performed using *H. comes* rather than *H. erectus* because of the more comprehensive gene annotation for *comes*.⁵² This genome provided 1:1 ortholog mapping between *H. comes* and *H. erectus*. Differential expression analysis between the three groups (paired males [PM] vs. unpaired males [UPM], paired males [PM] vs. paired females [PF], unpaired males [UPM] vs. paired females [PF]) was performed in R⁵³ using the limma voom pipeline,^{54,55} which consisted of normalization for factors such as sex and date of RNA extraction, statistical testing, and multiple testing correction using the Benjamini-Hochberg procedure.⁵⁶ No genes reached a statistically significant threshold (adjusted *p*-value <0.05) in any of the three pairwise comparisons.

Our analysis of RNAseq data consisted of three nonoverlapping lines of inquiry. The first analysis was a qualitative assessment of the number of up- or downregulated genes between experimental groups. The second analysis examined the gene ontology (GO) Annotations that were enriched in differentially expressed genes. The third line of inquiry employed the Rank-Rank Hypergeometric Analysis to compare gene expression in the brains of seahorses and another monogamous species, prairie voles (*Microtus ochrogaster*).

2.7 | Number of up- or downregulated genes

The expression of individual genes was normalized by calculating the Z-score of each gene for each individual ($Z = (x_1 - \bar{x})/\sigma$) then averaging Z-scores within a group (i.e., PM, PF and UPM). Genes were ranked within a group by Z-score, and we quantified the number of genes with a Z-score greater than 1 or less than -1. Z-scores greater than 1 represented upregulated gene activity compared to the population mean, and Z-scores less than -1 represented downregulated gene activity compared to the population mean. This analysis provided a global overview of how many genes were up- or downregulated in the three groups but was not meant to identify statistically significant changes in gene expression.

We also examined genes that are related to neurotransmitter systems that are classically associated with affiliative behaviors, including the nonapeptides OT/IT (oxt, oxtr, oxtrl) and arginine vasopressin/vasotocin (avp, avpr1a, avpr2a), opioid receptors (oprm1, oprk1,

oprd1b), dopamine (drd1, drd1b, drd2a, drd2l, drd3, drd4a, drd4b, drd6b) and serotonin (htr1a, htr1b, htr1ab, htr1f, htr2a, htr2b, htr2cl1, htr3a, htra3a, htr4, htr5ab, htr6, htr7a).

2.8 | Gene ontology analysis

Pathway enrichment analysis was conducted using GO terms and KEGG pathway annotations. The Kolmogorov-Smirnov test⁵⁷ was used to identify significantly enriched GO terms in topGO⁵⁸ (v2.44.0) while enriched pathways were deduced using the Wilcoxon rank-sum test⁵⁹ in KEGGREST (v1.32.0).⁶⁰

Individual genes are associated with GO annotations in order to describe the various functions of a particular gene product. The biological process analysis describes a recognized series of events or collection of molecular functions associated with a gene or gene product. The molecular function analysis describes the function that each gene product performs within the cell. The cellular component analysis describes the locations of gene expression, at the levels of subcellular structures. Each analysis was completed for all genes with differential patterns of expression between the three comparison groups, paired males (*n* = 3) versus unpaired males (*n* = 4) (PM vs. UPM), paired males versus paired females (*n* = 3) (PM vs. PF) and paired females versus unpaired males (PF vs. UPM). For this analysis we examined differentially expressed annotated transcripts with an uncorrected *p*-value <0.05. We identified GO annotations that were significantly enriched (false discovery rate <0.05) and selected the genes associated with those annotations for further examination.

2.9 | Rank-rank hypergeometric analysis

We compared orthologous gene expression between the medial preoptic area (MPOA) of unpaired and paired male prairie voles,⁶¹ the nucleus accumbens (NAcc) of unpaired and 3-week paired male prairie voles,⁶² and the whole brains of unpaired and paired male seahorses, using the Rank-Rank Hypergeometric Overlap (RRHO) algorithm. This approach identifies differentially expressed genes in a sample, ranks them in a list according to their log-fold change, and then compares that ranked list to lists from other datasets. RRHO has several advantages over more traditional direct comparisons of gene lists.⁶³ First, RRHO treats each list of differentially expressed genes as a continuous dataset, which avoids arbitrary significance cutoffs. Second, many genes will show coordinated patterns of altered expression, which can be difficult to detect using more traditional methods, but RRHO can identify these. Third, RRHO allows for the direct comparison of ranked lists generated by multiple datasets, which can allow researchers to identify trends in gene expression that may be difficult to find otherwise.

Of the starting list of expressed genes for each species (12,796 for seahorse whole brains, 14,363 for vole MPOA, and 19,647 for vole NAcc), 5918 genes were shared by seahorses and vole MPOA, 5678 were shared by seahorses and vole NAcc and 11,667 were shared by

vole MPOA and vole NAcc. We used the RRHO approach to assess whether the degree of overlap in gene expression for the shared genes was significant.^{63,64} We used the RRHO function from the “RRHO” package to compare the gene expression lists.⁶⁵ The resulting heatmap shows statistically significant overlap for gene signatures in each pairwise comparison. The analysis was conducted in R.⁵³

3 | RESULTS

3.1 | Baseline luminance and change during social interactions

We examined changes in luminance during a preference test as a potential indicator of social preference and behavioral synchrony between pair mates. The baseline luminance of both focal male and female seahorses was very similar during moments of no color change: Cohen's $d = 0.24$; mean \pm SE: $6.921\% \pm 0.048$ for females (unit is light reflectance in the luminance channel), and $6.780\% \pm 0.037$ for males. Similar levels of baseline luminance were also observed for both partner (Cohen's $d = 0.15$; mean \pm SE: $6.909\% \pm 0.058$ for females and $7.016\% \pm 0.053$ for males) and stranger male and female seahorses (Cohen's $d = 0.36$; mean \pm SE: $6.689\% \pm 0.040$ for females and $6.512\% \pm 0.034$ for males).

We registered a higher number of visual luminance changes when focal animals, both male and female, were in mutual proximity with their partner, compared to when they were in mutual proximity with the stranger (Table 2). Almost all the luminance changes observed during mutual interactions were performed by the partner male (when females were the focal individual) and the focal male (when males were the focal individual). Only five events of synchronous luminance change were observed, all during mutual interactions, with the change of the male being followed by a change in the female within a relatively short delay (mean \pm SE: 12.80 ± 6.25 s).

Although less numerous, the events of luminance change during non-mutual interactions (those in which the focal animal was in the partner or stranger zone, but the stimulus animal was distant from the focal animal) followed the same pattern as described for mutual interactions, with almost all color changes being made by the males (either as the focal male or as the partner). Interestingly, there were more events of non-mutual luminance change registered when focal seahorses of both sexes were close to the stranger side compared to the partner side (Table 2).

Generally, males showed a larger % luminance change than females. When focal males mutually interacted with their female partners, they showed a $20.08\% \pm 3.28$ luminance increase while the female partners showed a $7.24\% \pm 1.25$ luminance increase (Cohen's $d = 2.98$; Figure 2, Table 3). When focal males mutually interacted with stranger females, the focal males showed a $13.82\% \pm 6.38$ luminance increase while the female strangers showed a $1.22\% \pm 0.61$ luminance increase (Cohen's $d = 1.97$). The focal males appeared to distinguish between the partner and stranger, as the % luminance change of the focal male appeared somewhat higher when he was mutually interacting with the partner female, compared to when he was interacting with the stranger female (Cohen's $d = 0.83$; mean \pm SE: $20.08\% \pm 3.28$ for partner interaction and $13.82\% \pm 6.38$ for stranger interaction).

When focal females mutually interacted with their male partners, they showed an $8.61\% \pm 6.09$ luminance increase, while the male partners showed a $37.66\% \pm 18.29$ luminance increase (Cohen's $d = 1.51$; Figure 2, Table 3). When focal females mutually interacted with stranger males, the females showed a $4.63\% \pm 0.31$ luminance increase while the male strangers showed a $2.54\% \pm 0.61$ luminance increase (Cohen's $d = 3.05$). The focal females showed a slight increase in % luminance change when interacting with the male partner compared to the male stranger (Cohen's $d = 0.65$; mean \pm SE: $8.61\% \pm 6.09$ for partner interaction and $4.63\% \pm 0.31$ for stranger interaction).

TABLE 2 Total number of luminance change events observed in female and male seahorses during mutual (i.e., when the focal seahorse was located within the zone of interaction, close to the respective partner or stranger individual of the opposite sex) and non-mutual interactions (i.e., when the focal seahorse was located close to the divider wall, but the partner or stranger individual was positioned distant from the interaction zone) during a partner preference test (PPT). Table rows indicate the side of the tank (partner or stranger sides) where the interaction between the focal subject and the opposite-sex seahorse occurs, while the table columns show the subject in which the luminance change event was registered, being the female or male focal seahorses or the corresponding partner (P male—partner male; P female—partner female) and stranger (S male—stranger male; S female—stranger female) subjects. Synchronous (Sync) events of luminance change were defined by an event that was initiated by the partner male and followed by a subsequent change in the focal female seahorse

	Mutual proximity									
	Female subject	P male	S male	Sync	Total	Male subject	P female	S female	Sync	Total
Partner	0	26	0	4	30	22	1	0	0	23
Stranger	0	4	0	0	4	5	1	0	1	7
	Non-mutual location									
	Female subject	P male	S male	Sync	Total	Male subject	P female	S female	Sync	Total
Partner	0	1	0	0	1	2	0	0	0	0
Stranger	1	20	0	0	21	8	0	0	0	8

3.2 | Comparison of gene expression patterns between groups

To begin to understand the underlying genetic mechanisms contributing to pair bonding behaviors, we assayed the transcriptomes of all

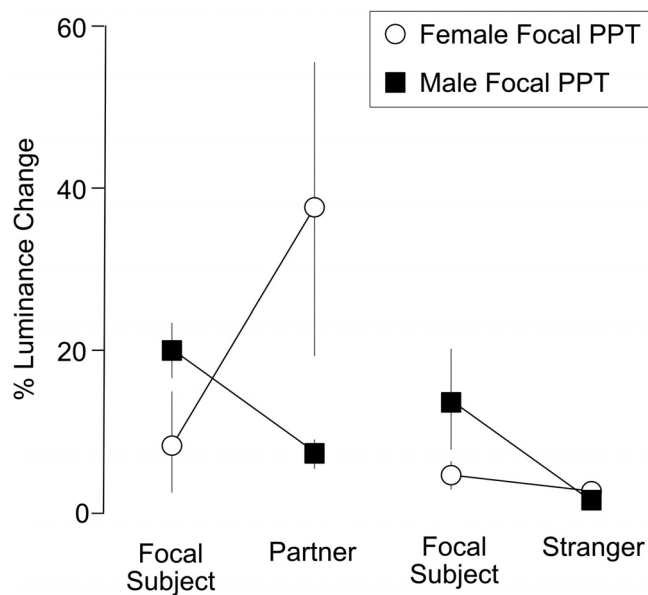


FIGURE 2 We examined mutual interactions during partner preference tests (PPT) between a focal seahorse and their partner or an opposite-sex stranger. For each interaction the maximum luminance was compared to the minimum luminance to calculate the % luminance change. In the female focal PPT (white circles) during focal subject/partner mutual interactions (left) the female subject showed a small increase in % luminance change, but less luminance change than her male partner, while during focal subject/stranger mutual interactions (right) both the female subject and the male stranger showed only a small luminance change. In the male focal PPT (black squares) the male subject showed a higher % luminance change than both the female partner during focal subject/partner mutual interactions (left) and the female stranger during focal subject/stranger mutual interactions (right). Mean ± SE

TABLE 3 Effect size (Cohen's *d*) of comparisons of change in luminance

	Fp	Fs	Mp	Ms
P	1.507	x	2.986	x
S	x	3.052	x	1.968
Fp	x	0.652	1.571	x
Fs	0.652	x	x	1.440
Mp	1.571	x	x	0.831
Ms	x	1.440	0.831	x

Abbreviations: Fp, focal female in mutual interaction with male partner; Fs, focal female in mutual interaction with male stranger; Mp, focal male in mutual interaction with female partner; Ms, focal male in mutual interaction with female stranger; P, partner in mutual interaction with focal subject; S, stranger in mutual interaction with focal subject; x, not tested.

tested subjects. Our RNA-seq analysis identified 20,788 transcripts; 15,200 were annotated to unique Ensembl IDs based on similarity to known genes in *H. comes*, sister species to *H. erectus* (diverged ~18.2 million years ago⁶⁶). No differentially expressed genes were found to be significant following adjustment for multiple comparisons. This was not surprising because of the small sample size, outbred nature of the subjects, and large phenotypic variability between subjects. However, it is important to emphasize that these results are describing trends and not statistically significant differences. Our analysis of RNAseq data consisted of three independent lines of inquiry described below.

We first examined all differentially expressed genes in all subjects to identify whether one group exhibited a greater number of differentially expressed genes than other groups. For each gene we calculated the z-score across three groups: PM, PF, UPM. We identified genes with z-scores above 1 and below -1 when compared to the population mean. By choosing this cutoff, we were focusing on the genes in the top 15.8% of each end of the distribution. We then counted the number of upregulated ($z > 1$) and downregulated ($z < -1$) genes in each group and determined whether they corresponded to an annotation (Figure 3). Paired females (PF, left) had the largest number of upregulated genes at 193, with 120 annotated (dark red) and 73 unannotated (light red), as well as 26 downregulated genes, including 20 annotated (dark blue) and 6 unannotated (light blue). Paired males (PM, center) had 65 upregulated genes, including 40 annotated

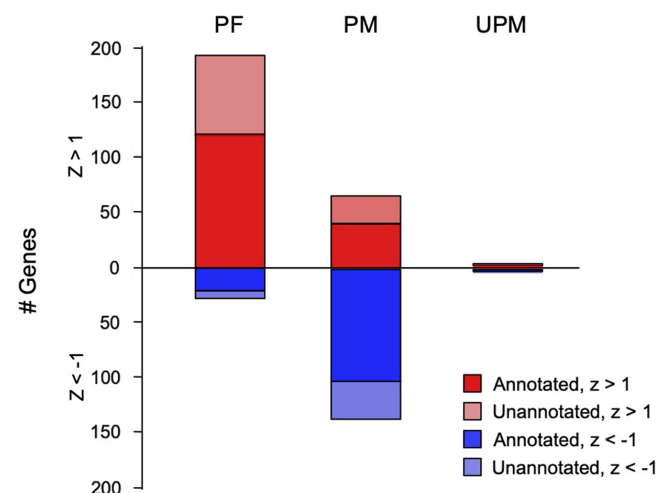


FIGURE 3 We calculated a z-score for each gene in each group (paired females [PF], left; paired males [PM], center; unpaired males [UPM], right), and determined the average z-score for each gene in each group. We identified the number of genes in each group with a z-score above 1 (red) or below -1 (blue), as well as the number of gene loci that were annotated (dark) or unannotated (light). PF seahorses had 193 genes (120 annotated and 73 unannotated) with a z-score above 1, and 26 genes (20 annotated and 6 unannotated) with a z-score below -1. PM seahorses had 65 genes (40 annotated and 25 unannotated) with a z-score above 1, and 137 genes (101 annotated and 36 unannotated) with a z-score below -1. UPM seahorses had 3 genes (2 annotated and 1 unannotated) with a z-score above 1, and 4 genes (1 annotated and 3 unannotated) with a z-score below -1.

TABLE 4 Gene ontology annotations comparing paired males and unpaired male seahorses. A list of differentially expressed genes was analyzed for their associated gene ontology annotations. We identified annotations with a false discovery rate <0.05 as well as the specific genes linked to those annotations

Gene ontology annotation	# Genes	Fold enrichment	False discovery rate	Gene IDs
Cilium organization (GO:0044782)	12	4.2	4.63E-02	wdpcp, cobl, tmem237a, mns1, tbc1d32, bbs4, cxcr4a, ttc8, pcdh15a, cfap206, ift27
Cellular component biogenesis (GO:0044085)	34	2.24	1.71E-02	cox17, kctd7, myot, cobl, srpk3, uqcc1, mphosph6, vamp2, tmem237a, pop1, dmtn, at12, tbc1d32, muc13b, bbs4, cxcr4a, nat10, tdrd1, ttc8, HSP90AA1, npas4a, nck2a, pcdh15a, clp1, exosc3, nol10, parvg, sfswap, cfap206, eif3jb, ift27, h1-0, dnaaf2, mylka
Cellular component assembly (GO:0022607)	30	2.23	5.00E-02	cox17, kctd7, myot, cobl, srpk3, uqcc1, vamp2, tmem237a, pop1, dmtn, at12, tbc1d32, muc13b, bbs4, cxcr4a, tdrd1, ttc8, HSP90AA1, npas4a, nck2a, pcdh15a, clp1, parvg, sfswap, cfap206, eif3jb, ift27, h1-0, dnaaf2, mylka
Primary metabolic process (GO:0044238)	92	1.61	2.46E-03	bdh2, psat1, dohh, fancd2, pkn2, rhbdl3, trrap, pigb, apip, mterf2, adat1, SMURF2, hipk2, tk1, pparaa, srpk3, smc5, ube3a, camk1db, mphosph6, aasdh, mapkapk3, tonsl, setd7, lipea, dusp3a, slc27a1a, zgc:163098, sgsh, erap1b, ube2t, TYR, b4galnt1a, tlk1a, rad17, prxl2b, ptpn21, trmt61b, ints2, aas, cars2, nek10, yrk, sgpl1, pkn2, bbs4, acy1, nat10, camkk1a, mst1, tdrd1, cadm1b, pla2g6, ddx1, hmces, mapk1, acox3, rad51d, peak1, igf1ra, exd3, clp1, pop1, exosc3, ptpn11a, rpl19, ehadh, nol10, gtpbp1, phka2, map4k5, sfswap, ice2, ext2, mgme1, nudt1, mmp19, mmp14b, ube2v1, usp12b, eif3jb, pglis, rnf141, tgm1l4, polr2c, bmp1rb, pcmtl, wdsb1, SGK3, mylka, dpp9
Nitrogen compound metabolic process (GO:0006807)	84	1.61	4.32E-03	bdh2, psat1, dohh, fancd2, pkn2, rhbdl3, trrap, pigb, apip, mterf2, adat1, SMURF2, hipk2, tk1, srpk3, smc5, ube3a, camk1db, mphosph6, mapkapk3, tonsl, setd7, dusp3a, slc27a1a, zgc:163098, sgsh, erap1b, ube2t, TYR, b4galnt1a, tmlhe, tlk1a, rad17, ptpn21, trmt61b, ints2, aas, cars2, nek10, yrk, sgpl1, pkn2, bbs4, acy1, nat10, camkk1a, mst1, tdrd1, ddx1, hmces, mapk1, rad51d, peak1, igf1ra, exd3, bckdhh, clp1, pop1, exosc3, ptpn11a, rpl19, nol10, gss, gtpbp1, map4k5, sfswap, ice2, ext2, mgme1, nudt1, mmp19, mmp14b, ube2v1, usp12b, eif3jb, rnf141, tgm1l4, polr2c, bmp1rb, pcmtl, wdsb1, SGK3, mylka, dpp9
Macromolecule metabolic process (GO:0043170)	74	1.6	2.62E-02	bdh2, dohh, fancd2, pkn2, rhbdl3, trrap, pigb, mterf2, adat1, SMURF2, hipk2, tk1, srpk3, smc5, ube3a, camk1db, mphosph6, mapkapk3, tonsl, setd7, dusp3a, zgc:163098, sgsh, erap1b, ube2t, tlk1a, rad17, ptpn21, trmt61b, ints2, cars2, nek10, yrk, pkn2, bbs4, nat10, camkk1a, mst1, tdrd1, ddx1, hmces, mapk1, rad51d, peak1, igf1ra, clp1, pop1, exosc3, ptpn11a, tprb, rpl19, nol10, gtpbp1, phka2, map4k5, sfswap, ice2, ext2, mgme1, nudt1, mmp19, mmp14b, ube2v1, usp12b, eif3jb, rnf141, tgm1l4, polr2c, bmp1rb, pcmtl, wdsb1, SGK3, mylka, dpp9
Cellular metabolic process (GO:0044237)	92	1.59	2.05E-03	bdh2, psat1, dohh, fancd2, pkn2, fra10ac1, trrap, pigb, apip, mterf2, adat1, SMURF2, hipk2, tk1, pparaa, srpk3, smc5, ube3a, camk1db, mphosph6, aasdh, mapkapk3, tonsl, setd7, lipea, dusp3a, slc27a1a, zgc:163098, sgsh, erap1b, ube2t, COX2, TYR, slc25a18, b4galnt1a, tmlhe, tlk1a, rad17, prxl2b, ptpn21, trmt61b, ints2, aas, cars2, nek10, yrk, sgpl1, pkn2, bbs4, acy1, nat10, camkk1a, tdrd1, pla2g6, ddx1, hmces, mapk1, acox3, rad51d, peak1, igf1ra, exd3, bckdhh, clp1, cyp1a, pop1, exosc3, ptpn11a, rpl19, ehadh, nol10, gss, gtpbp1, phka2, map4k5, sfswap, ice2, ext2, mgme1, nudt1, ube2v1, usp12b, eif3jb, pglis, rnf141, tgm1l4, polr2c, bmp1rb, pcmtl, wdsb1, SGK3, mylka

(Continues)

TABLE 4 (Continued)

Gene ontology annotation	# Genes	Fold enrichment	False discovery rate	Gene IDs
Organic substance metabolic process (GO:0071704)	96	1.58	2.08E-03	bdh2, psat1, dohh, fancd2, pkn2, rhbdl3, trrap, pigb, apip, mterf2, adat1, SMURF2, hipk2, tk1, pparaa, srpk3, smc5, ube3a, camk1db, mphosph6, aasdh, mapkapk3, tonsl, setd7, lipea, dusp3a, slc27a1a, zgc:163098, sgsh, erap1b, ube2t, TYR, b4galnt1a, tmlhe, tlk1a, rad17, prxl2b, ptpn21, trmt61b, ints2, aass, cars2, nek10, yrk, sgpl1, pkn2, bbs4, acy1, nat10, camkk1a, mst1, tdrd1, cadm1b, pla2g6, ddx1, hmces, mapk1, acox3, rad51d, peak1, igf1ra, exd3, bckdhh, clip1, pop1, exosc3, ptpn11a, tprb, rpl19, ehhadh, nol10, gss, gtpbp1, phka2, map4k5, sfswap, ice2, ext2, mgme1, nudt1, mmp19, mmp14b, ube2v1, usp12b, eif3jb, pglis, rnf141, tgm1l4, polr2c, bmpr1bb, pcmtil, wdsusb1, SGK3, mylka, dpp9
Metabolic process (GO:0008152)	100	1.55	1.91E-03	bdh2, psat1, dohh, fancd2, pkn2, fra10ac1, rhbdl3, trrap, pigb, apip, mterf2, adat1, SMURF2, hipk2, tk1, pparaa, srpk3, smc5, ube3a, pcca, camk1db, mphosph6, aasdh, mapkapk3, tonsl, setd7, lipea, dusp3a, slc27a1a, zgc:163098, sgsh, erap1b, ube2t, COX2, TYR, slc25a18, b4galnt1a, tmlhe, tlk1a, rad17, prxl2b, ptpn21, trmt61b, ints2, aass, cars2, nek10, yrk, sgpl1, pkn2, bbs4, acy1, nat10, camkk1a, mst1, tdrd1, cadm1b, pla2g6, ddx1, hmces, mapk1, acox3, rad51d, peak1, igf1ra, exd3, bckdhh, clip1, cyp1a, pop1, exosc3, ptpn11a, tprb, rpl19, ehhadh, nol10, gss, gtpbp1, phka2, map4k5, sfswap, ice2, ext2, mgme1, nudt1, mmp19, mmp14b, ube2v1, usp12b, eif3jb, pglis, rnf141, tgm1l4, polr2c, bmpr1bb, pcmtil, wdsusb1, SGK3, mylka, dpp9
Cellular process (GO:0009987)	173	1.28	4.51E-03	bdh2, rem2, psat1, dohh, fancd2, wdpcp, pkn2, pde6a, cox17, fra10ac1, vt11b, trrap, kctd7, pigb, apip, mterf2, swap70b, adat1, myot, cobi, SMURF2, hipk2, chrnb3a, tk1, pparaa, srpk3, smc5, mfsd9, ube3a, UBL4A, prlrb, uqcc1, camk1db, dnah6, mphosph6, aasdh, slc7a11, mapkapk3, vampe2, tonsl, setd7, lipea, CPNE3, dusp3a, slc27a1a, zgc:163098, sgsh, erap1b, tmem237a, ube2t, COX2, svopb, pop1, TYR, slc25a18, b4galnt1a, cplx2l, sparta, tmlhe, tlk1a, dmtn, mns1, rad17, prxl2b, ptpn21, atl2, trmt61b, ints2, aass, tbc1d32, fer1l4, pdlim7, neurod2, cars2, nek10, yrk, sgpl1, pkn2, muc13b, bbs4, acy1, paqr8, cxc4a, dbx1a, thsd7aa, nat10, camkk1a, tdrd1, cadm1b, mic1, pla2g6, ddx1, slc6a2, MTSS1, hmces, syt1b, ABCC4, ttc8, HSP90AA1, DNAH10, mapk1, egr1, itgam, acox3, rad51d, tango6, peak1, igf1ra, alk1, npas4a, tbc1d22b, nck2a, pcdh15a, DNAJC15, exd3, bckdhh, clip1, cyp1a, pop1, exosc3, kitiga, ptpn11a, tprb, rpl19, ehhadh, nol10, gss, parvg, gtpbp1, pcdh2ab2, phka2, map4k5, tango6, eps15, sfswap, ice2, nmur3, kif4, ext2, mgme1, CHRNA9, nudt1, mmp19, cfap206, mmp14b, ube2v1, usp12b, dnah6, fam83fb, atp7b, eif3jb, pglis, MARF1, rnf141, myca, ift27, rasgrp3, stc1l, tgm1l4, polr2c, h1-0, bmpr1bb, efr3a, dhaaf2, robo1, pcmtil, wdsusb1, SGK3, abca4a, calb2a, mylka, itrp1a, ccdc88aa
Dynein light intermediate chain binding (GO:0051959)	4	17.57	3.05E-02	dnah6, DNAH10, ccdc88aa
Adenyl ribonucleotide binding (GO:0032559)	36	2.26	1.04E-02	pkn2, hipk2, tk1, srpk3, smc5, pcca, camk1db, dnah6, aasdh, mapkapk3, ube2t, pop1, tlk1a, rad17, cars2, nek10, yrk, pkn2, nat10, camkk1a, ddx1, ABCC4, HSP90AA1, DNAH10, mapk1, rad51d, peak1, igf1ra, clip1, gss, map4k5, atp7b, bmpr1bb, SGK3, abca4a, mylka

TABLE 4 (Continued)

Gene ontology annotation	# Genes	Fold enrichment	False discovery rate	Gene IDs
Adenyl nucleotide binding (GO:0030554)	36	2.25	7.44E-03	pkn2, hipk2, tk1, srpk3, smc5, pcca, camk1db, dnah6, aasdh, mapkapk3, ube2t, pop1, tik1a, rad17, cars2, nek10, yrk, pkn2, nat10, camkk1a, ddx1, ABCC4, HSP90AA1, DNAH10, mapk1, rad51d, peak1, igf1ra, clp1, gss, map4k5, atp7b, bmpr1bb, SGK3, abca4a, mylka
ATP binding (GO:0005524)	35	2.25	7.96E-03	pkn2, hipk2, tk1, srpk3, smc5, pcca, camk1db, dnah6, aasdh, mapkapk3, ube2t, tik1a, rad17, cars2, nek10, yrk, pkn2, nat10, camkk1a, ddx1, ABCC4, HSP90AA1, DNAH10, mapk1, rad51d, peak1, igf1ra, clp1, gss, map4k5, atp7b, bmpr1bb, SGK3, abca4a, mylka
Purine ribonucleotide binding (GO:0032555)	40	1.95	2.48E-02	rem2, pkn2, hipk2, tk1, srpk3, smc5, pcca, camk1db, dnah6, aasdh, mapkapk3, ube2t, pop1, tik1a, rad17, atl2, cars2, nek10, yrk, pkn2, nat10, camkk1a, ddx1, ABCC4, HSP90AA1, DNAH10, mapk1, rad51d, peak1, igf1ra, clp1, gss, gtpbp1, map4k5, atp7b, ift27, bmpr1bb, SGK3, abca4a, mylka
Purine ribonucleoside triphosphate binding (GO:0035639)	39	1.95	2.57E-02	rem2, pkn2, hipk2, tk1, srpk3, smc5, pcca, camk1db, dnah6, aasdh, mapkapk3, sgsh, ube2t, pop1, tik1a, rad17, atl2, cars2, nek10, yrk, pkn2, nat10, camkk1a, ddx1, ABCC4, HSP90AA1, DNAH10, mapk1, rad51d, peak1, igf1ra, clp1, gss, gtpbp1, map4k5, atp7b, ift27, bmpr1bb, SGK3, abca4a, mylka
Ribonucleotide binding (GO:0032553)	40	1.94	2.35E-02	rem2, pkn2, hipk2, tk1, srpk3, smc5, pcca, camk1db, dnah6, aasdh, mapkapk3, ube2t, pop1, tik1a, rad17, atl2, cars2, nek10, yrk, pkn2, nat10, camkk1a, ddx1, ABCC4, HSP90AA1, DNAH10, mapk1, rad51d, peak1, igf1ra, clp1, gss, gtpbp1, map4k5, atp7b, ift27, bmpr1bb, SGK3, abca4a, mylka
Purine nucleotide binding (GO:0017076)	40	1.93	2.22E-02	rem2, pkn2, hipk2, tk1, srpk3, smc5, pcca, camk1db, dnah6, aasdh, mapkapk3, ube2t, pop1, tik1a, rad17, atl2, cars2, nek10, yrk, pkn2, nat10, camkk1a, ddx1, ABCC4, HSP90AA1, DNAH10, mapk1, rad51d, peak1, igf1ra, clp1, gss, gtpbp1, map4k5, atp7b, ift27, bmpr1bb, SGK3, abca4a, mylka
Antion binding (GO:0043168)	45	1.92	1.54E-02	rem2, psat1, pkn2, zgc:85777, hipk2, tk1, srpk3, smc5, pcca, camk1db, dnah6, aasdh, mapkapk3, ube2t, pop1, tik1a, rad17, atl2, cars2, nek10, yrk, sgpl1, pkn2, nat10, camkk1a, ddx1, ABCC4, HSP90AA1, DNAH10, mapk1, acox3, rad51d, peak1, igf1ra, clp1, gss, gtpbp1, map4k5, atp7b, ift27, bmpr1bb, SGK3, abca4a, mylka, itpr1a
Small molecule binding (GO:0036094)	47	1.91	1.11E-02	rem2, psat1, pkn2, zgc:85777, hipk2, tk1, srpk3, smc5, pcca, camk1db, dnah6, aasdh, mapkapk3, ube2t, pop1, tik1a, rad17, atl2, OSBP2, cars2, nek10, yrk, sgpl1, pkn2, nat10, camkk1a, ddx1, OSBP2, ABCC4, HSP90AA1, DNAH10, mapk1, acox3, rad51d, peak1, igf1ra, clp1, gss, gtpbp1, map4k5, atp7b, ift27, bmpr1bb, SGK3, abca4a, mylka, itpr1a
Nucleotide binding (GO:0000166)	42	1.86	2.39E-02	rem2, pkn2, zgc:85777, hipk2, tk1, srpk3, smc5, pcca, camk1db, dnah6, aasdh, mapkapk3, ube2t, pop1, tik1a, rad17, atl2, cars2, nek10, yrk, pkn2, nat10, camkk1a, ddx1, ABCC4, HSP90AA1, DNAH10, mapk1, acox3, rad51d, peak1, igf1ra, clp1, gss, gtpbp1, map4k5, atp7b, ift27, bmpr1bb, SGK3, abca4a, mylka
Nucleoside phosphate binding (GO:1901265)	42	1.86	2.22E-02	rem2, pkn2, zgc:85777, hipk2, tk1, srpk3, smc5, pcca, camk1db, dnah6, aasdh, mapkapk3, ube2t, pop1, tik1a, rad17, atl2, cars2, nek10, yrk, pkn2, nat10, camkk1a,

(Continues)

TABLE 4 (Continued)

Gene ontology annotation	# Genes	Fold enrichment	False discovery rate	Gene IDs
Carbohydrate derivative binding (GO:0097367)	41	1.84	4.25E-02	ddx1, ABCC4, HSP90AA1, DNAH10, mapk1, acox3, rad51d, peak1, igf1ra, clp1, gss, gtpbp1, map4k5, atp7b, ift27, bmpr1bb, SGK3, abca4a, mylka rem2, pkn2, hipk2, tk1, srpk3, smc5, pcca, camk1db, dnah6, aasdh, mapkapk3, sgsh, ube2t, pop1, tlk1a, rad17, atf2, cars2, nek10, yrk, pkn2, nat10, camkk1a, ddx1, ABCC4, HSP90AA1, DNAH10, mapk1, rad51d, peak1, igf1ra, clp1, gss, gtpbp1, map4k5, atp7b, ift27, bmpr1bb, SGK3, abca4a, mylka
Catalytic activity (GO:0003824)	97	1.62	5.69E-04	bdh2, rem2, psat1, dohh, mettl27, pkn2, pde6a, fra10ac1, rhbdl3, trrap, pigb, apip, adatl1, zgc:85777, SMURF2, hipk2, tk1, ces2b, srpk3, ube3a, pcca, camk1db, dnah6, aasdh, mapkapk3, exd3, setd7, lipea, dusp3a, slc27a1a, sgsh, erap1b, ube2t, COX2, TYR, phospho2, b4galnt1a, trim36, tmlhe, tlk1a, rad17, prxl2b, ptpn21, atf2, trmt61b, aass, cars2, nek10, yrk, sgpl1, pkn2, acy1, nat10, camkk1a, mst1, cadml1b, pla2g6, ddx1, zgc:101858, hmces, ABCC4, DNAH10, mapk1, acox3, rad51d, peak1, igf1ra, glrx, exd3, tsnax, cyb561d1, bckdhh, clp1, cyp1a, ptpn11a, ehadh, gss, gtpbp1, map4k5, ext2, mgrme1, nudt1, mmp19, mmp14b, usp12b, dnah6, pgl, rnf141, ift27, tgm14, polr14, polr2c, bmpr1bb, pcmt1, wdsu1, SGK3, mylka, dpp9

(dark red) and 25 unannotated (light red), and 137 downregulated genes, including 101 annotated (dark blue) and 36 unannotated (light blue). In contrast, unpaired males (UPM, right) had 3 upregulated genes, including 2 annotated (dark red) and 1 unannotated (light red) and 4 downregulated genes, including 1 annotated (dark blue) and 3 unannotated (light blue).

We specifically examined the expression of genes that have been linked to pair bonding, including those in the nonapeptide, dopamine, opioid, and serotonin systems. We found two genes out of 30 with a z-score >1: Oxt1 in PF, and Htr4 in PM. We found no changes in the expression of genes related to the dopaminergic or opioid systems.

Next, we compared gene expression across three groups (PM vs. UPM, PM vs. PF and PF vs. UPM) identifying different patterns of gene expression and assessed if common biological, molecular, and cellular functions existed for differentially expressed genes between the three comparison groups using GO analysis (see Methods). Focusing on GO annotations with false-discovery rate less than 0.05, we identified 25 annotations of differentially expressed genes between the PM versus UPM condition primarily related to metabolic processes, cellular processes, nucleotide binding and catalytic activity (see Table 4 for a complete list of GO annotations and associated genes). One annotation was identified for the differential genes expressed in the PM versus PF condition, which was related to cellular nitrogen compound metabolic processes (see Table 5 for a list of GO annotations and associated genes), while no GO annotations were identified for genes differentiating the PF versus UPM condition. Of the 182 PM versus UPM differentially expressed genes included as significant in GO annotations, 58 genes were associated with 67 Kegg pathways (Table 6), with the most commonly recurring pathways including those related to metabolism, calcium, MAPK, GnRH and FoxO signaling, apoptosis, as well as RNA degradation, polymerase, and transport pathways.

3.3 | RRHO analysis

We next sought to compare if underlying mechanisms may converge between separate sets of pair bonding organisms by performing a RRHO analysis, an approach used to compare the gene expression of subjects in different experiments that have experienced similar experimental conditions. It is designed to be used to compare gene expression both between species and between studies,^{63,64} and has recently been used to compare gene expression in multiple monogamous species in order to suggest genes that may be conserved across phylogenies.¹⁶ In this analysis, we compared differentially expressed genes in lined seahorses to data from a previous study where we examined gene expression in male prairie voles that had experienced one of three parenting conditions: virgin males, paired males and males with fathering experience.⁶¹ We also compared both seahorse and prairie vole MPOA gene expression data to gene expression from a previously published prairie vole study,⁶² which contained publicly available data from the NAcc of male prairie voles that had experienced 3 weeks of cohabitation with a partner (3 W)⁶² compared to males

TABLE 5 Gene ontology annotations of differentially expressed genes identified by comparing paired males and paired female seahorses. A list of differentially expressed genes was analyzed for their associated gene ontology annotations. We identified annotations with a false discovery rate <0.05 as well as the specific genes linked to those annotations

Gene ontology annotation	# Genes	Fold enrichment	False discovery rate	Gene IDs
Cellular nitrogen compound metabolic process (GO:0034641)	43	2.1	3.33E-02	rbm10, gtf2a1l, ak7b, mrpl43, nme5, tk1, tet1, smc5, smarcal1, rtraf, zranb3, erap1b, exosc10, ube2t, b4galnt1a, rad51b, mrpl15, acaca, spout1, ybx1, eif4e3, cars2, clic1, pusl1, pcid2, tdrd1, mpv17, ddx1, ints4, exd3, cers5, rad50, pop1, gtf3c2, gtpbbp1, atp5f1e, ice2

TABLE 6 Kegg pathway analysis for differentially expressed genes identified by comparing paired male versus unpaired male groups. Genes that were linked to significantly enriched gene ontology annotations were analyzed for their association with Kegg pathways

Kegg pathway	Genes
Apoptosis/Ferroptosis/cellular senescence	itpr1a, mapk1, neurod2, slc7a11, gss, hipk2
Arginine biosynthesis	acy1
Biosynthesis of amino acids/cofactors	psat1, acy1, gss, phospho2
Calcium signaling pathway	itpr1a, mst1
Carbon metabolism	pcca, pgl5, psat1
Cell adhesion molecules	egr1, itgam
Cysteine and methionine metabolism	gss, psat1, apip
FoxO signaling pathway	mst1, setd7, SGK3
Gap junction	itpr1a
GnRH signaling pathway	egr1, itpr1a, mapk1
MAPK signaling pathway	mapk1, mapkapk3, mst1, rasgrp3
Metabolic pathways	myca, nudt1, pcca, pgl5, phospho2, pigb, psat1, setd7, sgpl1, sgsh, tmlhe, ube2v1, aass, acox3, acy1, apip, bckdhd, bdh2, COX2, ehhadh, ext2, gss,
RNA degradation/polymerase/transport	mphosph6, nudt1, exosc3, polr2c, pop1

that cohabitated with a same-sex sibling (SN). We chose to compare the PM versus UPM seahorse data against the virgin versus paired male prairie vole MPOA data⁶¹ and the SN versus 3 W vole NAcc data,⁶² as these subjects experienced the most analogous experimental conditions. For each species, the differentially expressed genes were placed in rank-order based on log-fold change of expression. Then those lists were compared against each other. When individual genes were in similar places in each list, we concluded that those genes were similarly expressed in each species. The resulting heat map indicates locations where genes co-occur in both lists, with brighter colors indicating greater similarities between gene lists.

Figure 4 shows the results of the three pairwise RRHO analyses. The top row shows heat maps generated by the comparison of gene

expression in seahorse whole brain and prairie vole MPOA (A), seahorses and prairie vole NAcc (D), and prairie vole MPOA and prairie vole NAcc (G). The top right corner represents significant overlap between genes that are upregulated in both species, while the bottom left corner represents significant overlap between genes that are downregulated in both species. The middle row depicts Venn diagrams comparing the number of genes that were upregulated in (B) seahorses (blue) and prairie vole MPOA (red), (E) seahorses (blue) and prairie vole NAcc (yellow), and (H) prairie vole MPOA (red) and prairie vole NAcc (yellow). The bottom row depicts Venn diagrams comparing the number of genes that were downregulated in (C) seahorses (blue) and prairie vole MPOA (red), (F) seahorses (blue) and prairie vole NAcc (yellow), and (I) prairie vole MPOA (red) and prairie vole NAcc (yellow).

Comparisons of differentially expressed genes between virgin and paired male seahorses and prairie vole MPOA showed 150 upregulated genes and 90 downregulated genes (Supplementary Table 1) significantly overlapping between seahorses and prairie voles. Comparisons of seahorses to prairie vole NAcc showed 38 upregulated genes and 76 downregulated genes (Supplementary Table 1). Genes upregulated in both species were associated with several biological functions, including DNA/RNA activity, cell cycle, actin cytoskeleton, metabolic processes, ion channel/receptor, hormones, metal ion binding, and cilia, with shared downregulated genes involved in many of these same processes. This is likely a result of the fact that activation of a gene can potentially have activational or inhibitory effects on a given biological process. Thus, the fact that similar processes are represented in populations of both upregulated and downregulated genes reinforces the validity of this analysis.

We next examined the GO Annotations associated with the up- and downregulated genes identified in the RRHO analysis. We found zero GO annotations that were associated with upregulated genes in either the seahorse/prairie vole MPOA comparison or the seahorse/prairie vole NAcc comparison. However, we found 37 GO annotations that were associated with downregulated genes in the seahorse/prairie vole MPOA comparison (Table 7). These GO annotations include DNA replication (GO:0006260), multicellular organismal homeostasis (GO:0048871), cellular response to stress (GO:0033554), and binding (GO:0005488). Additionally, we identified nine GO annotations that were associated with downregulated genes in the seahorse/prairie vole NAcc comparison (Table 8). These GO annotations were predominantly associated with cilia and include cilium

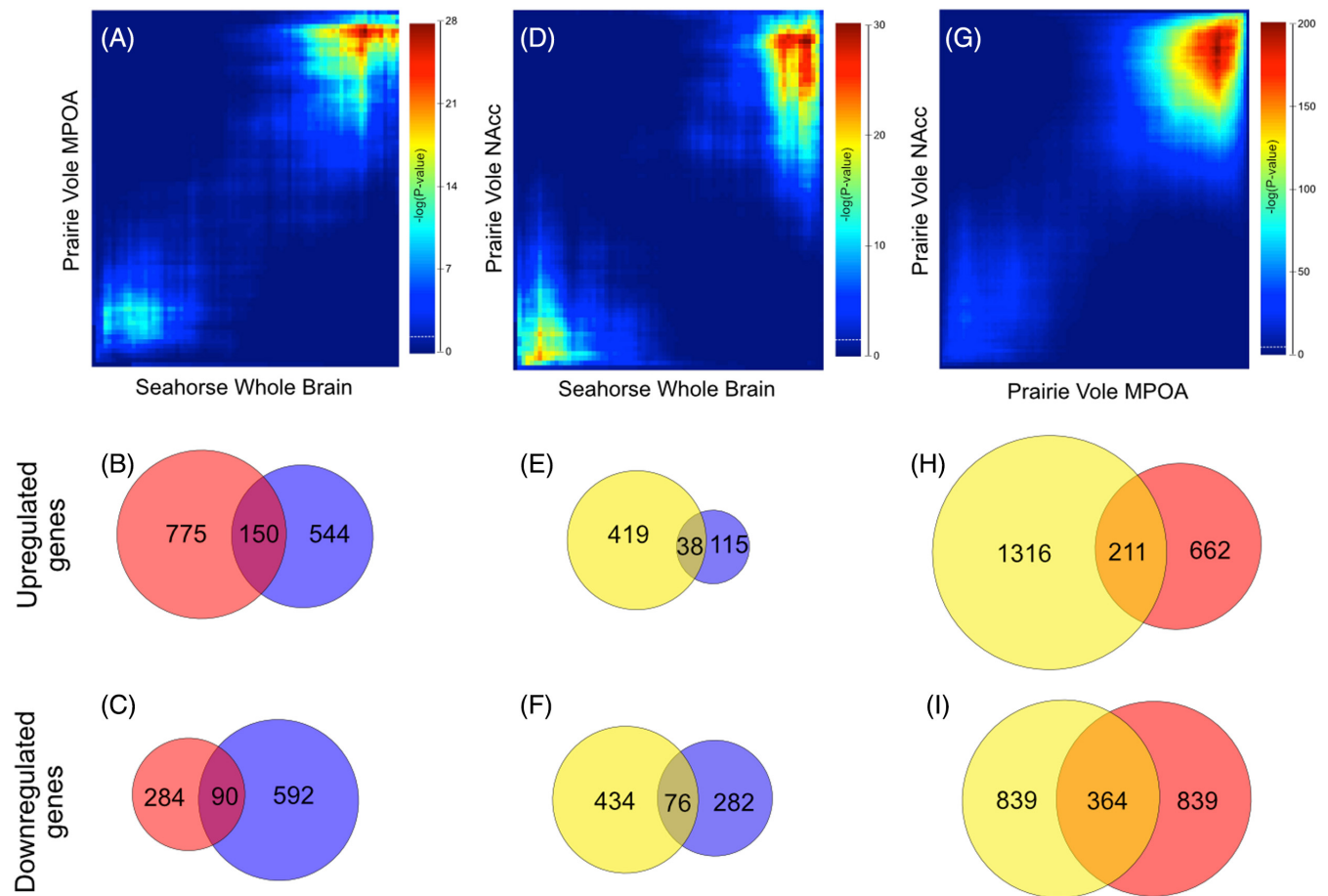


FIGURE 4 We used a rank–rank hypergeometric analysis (RRHO) to compare differentially expressed genes from the whole brains of lined seahorses and the MPOA and NAcc of prairie voles. The RRHO generates a heat map with the color of each pixel representing the enrichment of overlapping gene groups from the different species (A, D, G). Values in the heatmap are the corrected false discovery rate log transformed hypergeometric p -value for the likelihood of observing the given number of overlapping genes between the two rank thresholds along the plot. The top right quadrant represents genes that are upregulated in both species, while the bottom left quadrant represents genes that are downregulated in both species. Heat map scale = $-\log_{10}(P\text{-value})$. The dashed white line represents the color value where $p = 0.05$. (B) Venn diagram showing the number of upregulated genes in prairie vole MPOA (775; red), lined seahorse whole brain (544; blue), and the number of shared upregulated genes (150; purple). (C) Venn diagram showing the number of downregulated genes in prairie vole MPOA (284; red), lined seahorse whole brain (592; blue), and the number of shared downregulated genes (90; purple). (E) Venn diagram showing the number of upregulated genes in prairie vole NAcc (419; yellow), lined seahorse whole brain (115; blue), and the number of shared upregulated genes (38; green). (F) Venn diagram showing the number of downregulated genes in prairie vole NAcc (434; yellow), lined seahorse whole brain (282; blue), and the number of shared upregulated genes (76; green). (H) Venn diagram showing the number of upregulated genes in prairie vole NAcc (1316; yellow), prairie vole MPOA (662; red), and the number of shared upregulated genes (211; orange). (I) Venn diagram showing the number of downregulated genes in prairie vole NAcc (839; yellow), prairie vole MPOA (839; red), and the number of shared upregulated genes (364; orange). MPOA, medial preoptic area; NAcc, nucleus accumbens

movement (GO:0003341), ciliary plasm (GO:0097014) and cytoplasmic region (GO:0099568).

4 | DISCUSSION

This pilot study is one of the first explorations of social communication of paired lined seahorses in a laboratory setting. Changes in luminance present an exciting opportunity to study social communication and coordination in seahorses. Our results indicate a large role for the male in this mode of signaling, which was directed preferentially

toward his partner rather than toward the stranger female. As focal animals, males changed color a total of 24 times on their partner's side of the tank and 13 times on the stranger side; as either partner or focal males, males changed color a total of 48 times when in mutual proximity to their partner and only five times in mutual proximity to the stranger. Males also showed greater maximum luminance to their partner than to the stranger female.

Females changed color much less overall than males. Female color change events were also skewed toward the pair mate—with most changes (4 of 5 as the focal animal) being synchronous changes with the pair mate, in which the male pair mate changed first. Males had

TABLE 7 Gene ontology annotations for downregulated genes identified through the comparisons of seahorse and vole MPOA using RRHO. The RRHO analysis identified genes that were downregulated in both the seahorse brain and prairie vole MPOA. We analyzed these genes for their associated gene ontology annotations. We identified annotations with a false discovery rate <0.05 as well as the specific genes linked to those annotations

Gene ontology annotation	# Genes	fold enrichment	False discovery rate	Genes
DNA-dependent DNA replication (GO:0006261)	6	12.15	1.75E-02	Recql, Pold1, Mcm10, Primpol, Orc1, Rfc4
Response to UV (GO:0009411)	6	9.62	4.64E-02	Nfatc4, Ddb2, Chek1, Casp7, Pold1, Primpol
DNA replication (GO:0006260)	7	9.4	1.78E-02	Recql, Chtf18, Pold1, Mcm10, Primpol, Orc1, Rfc4
Tissue homeostasis (GO:0001894)	8	8.31	1.56E-02	Mks1, Nphp3, Enpp1, Sash3, Klhl10, Rbp4, Kdr, Comp
Anatomical structure homeostasis (GO:0060249)	8	7	2.42E-02	Mks1, Nphp3, Enpp1, Sash3, Klhl10, Rbp4, Kdr, Comp
Response to light stimulus (GO:0009416)	9	6.7	1.54E-02	Nfatc4, Ddb2, Chek1, Casp7, Reep6, Abca7, Pold1, Primpol, Rbp4
Multicellular organismal homeostasis (GO:0048871)	10	6.36	1.51E-02	Mks1, Nphp3, Enpp1, Sash3, Trpm2, Klhl10, Rbp4, Kdr, Comp, Alox12
Response to radiation (GO:0009314)	10	5.57	1.65E-02	Nfatc4, Ddb2, Chek1, Casp7, Reep6, Abca7, Pold1, Primpol, Rbp4, Eya1
Heart development (GO:0007507)	13	5.4	7.61E-03	Mks1, Nfatc4, Nphp3, Enpp1, Pdgfb, Mst1, Casp7, Pkd2, Hspb7, Rbp4, Kdr, Eya1, Adap2
DNA metabolic process (GO:0006259)	13	4.79	1.41E-02	Ddb2, Recql, Chek1, Cdc7, Tert, Chtf18, Msh3, Pold1, Mcm10, Primpol, Orc1, Eya1, Rfc4
Cellular response to DNA damage stimulus (GO:0006974)	13	4.52	1.74E-02	Ddb2, Nfatc4, Foxo4, Recql, Chek1, Lyn, Cdc7, Msh3, Pold1, Mcm10, Primpol, Eya1, Rfc4
Response to abiotic stimulus (GO:0009628)	18	4.43	1.82E-03	Ddb2, Nfatc4, Chek1, Tert, Casp7, Reep6, Abca7, Pkd2, Dysf, Trpm2, Hspb7, Pold1, Tbl2, Kcnk4, Primpol, Rbp4, Kdr, Eya1
Tube morphogenesis (GO:0035239)	13	4.22	1.65E-02	Mks1, Nfatc4, Nphp3, Enpp1, Pdgfb, Mst1, Pkd2, Dysf, Mst1, Bmper, Kdr, Eya1, Comp
Circulatory system development (GO:0072359)	16	4.09	9.34E-03	Mks1, Nfatc4, Nphp3, Enpp1, Pdgfb, Mst1, Casp7, Pkd2, Dysf, Hspb7, Bmper, Rbp4, Kdr, Eya1, Comp, Adap2
Tube development (GO:0035295)	14	3.49	4.50E-02	Mks1, Nfatc4, Nphp3, Enpp1, Pdgfb, Mst1, Pkd2, Dysf, Mst1, Bmper, Kdr, Eya1, Comp, Rbp4
Cellular response to stress (GO:0033554)	19	3.11	1.56E-02	Ddb2, Nfatc4, Enpp1, Foxo4, Recql, Chek1, Lyn, Cdc7, Tert, Pkd2, Dysf, Trpm2, Msh3, Pold1, Tbl2, Mcm10, Primpol, Eya1, Rfc4
Regulation of cell population proliferation (GO:0042127)	21	2.9	1.64E-02	Ptafr, Mks1, Pdgfb, Foxo4, Mst1, Chek1, Lyn, Cdc7, Tert, Sash3, Pkd2, Dysf, Mst1, Zbtb49, Rbp4, Kdr, Orc1, Eya1, Comp, Alox12, Npy
Organic substance biosynthetic process (GO:1901576)	22	2.49	4.39E-02	Ptafr, Rpl5, Has1, Asah2, Enpp1, Recql, Pccr, Lyn, Lpl, Tert, Pygl, Mrps10, Chtf18, Pold1, Mcm10, Thap1, Primpol, Rbp4, Orc1, Rfc4, Alox12, Ears2
Phosphoglucomutase activity (GO:0004614)	2	> 100	4.57E-02	Pgm1, Pgm2

(Continues)

TABLE 7 (Continued)

Gene ontology annotation	# Genes	fold enrichment	False discovery rate	Genes
ATP binding (GO:0005524)	18	3.08	1.13E-02	Irak3, Enpp1, Sgk3, Mst1, Recql, Chek1, Lyn, Cdc7, Pygl, Abca7, Abcc12, Chtf18, Msh3, Plk4, Kdr, Orc1, Rfc4, Ears2
Adenyl ribonucleotide binding (GO:0032559)	18	2.93	1.34E-02	Irak3, Enpp1, Sgk3, Mst1, Recql, Chek1, Lyn, Cdc7, Pygl, Abca7, Abcc12, Chtf18, Msh3, Plk4, Kdr, Orc1, Rfc4, Ears2
Adenyl nucleotide binding (GO:0030554)	18	2.9	1.39E-02	Irak3, Enpp1, Sgk3, Mst1, Recql, Chek1, Lyn, Cdc7, Pygl, Abca7, Abcc12, Chtf18, Msh3, Plk4, Kdr, Orc1, Rfc4, Ears2
Carbohydrate derivative binding (GO:0097367)	26	2.85	1.65E-03	Ptafr, Ndor1, Irak3, Rab32, Enpp1, Sgk3, Mst1, Recql, Chek1, Lyn, Lpl, Cdc7, Rasef, Pygl, Abca7, Abcc12, Trpm2, Chtf18, Msh3, Hapln2, Plk4, Kdr, Orc1, Comp, Rfc4, Ears2
Purine ribonucleoside triphosphate binding (GO:0035639)	20	2.77	1.43E-02	Irak3, Rab32, Enpp1, Sgk3, Mst1, Recql, Chek1, Lyn, Cdc7, Rasef, Pygl, Abca7, Abcc12, Chtf18, Msh3, Plk4, Kdr, Orc1, Rfc4, Ears2
Ribonucleotide binding (GO:0032553)	21	2.75	1.23E-02	Ndor1, Irak3, Rab32, Enpp1, Sgk3, Mst1, Recql, Chek1, Lyn, Cdc7, Rasef, Pygl, Abca7, Abcc12, Chtf18, Msh3, Plk4, Kdr, Orc1, Rfc4, Ears2
Purine ribonucleotide binding (GO:0032555)	20	2.65	1.63E-02	Irak3, Rab32, Enpp1, Sgk3, Mst1, Recql, Chek1, Lyn, Cdc7, Rasef, Pygl, Abca7, Abcc12, Chtf18, Msh3, Plk4, Kdr, Orc1, Rfc4, Ears2
Purine nucleotide binding (GO:0017076)	20	2.63	1.71E-02	Irak3, Rab32, Enpp1, Sgk3, Mst1, Recql, Chek1, Lyn, Cdc7, Rasef, Pygl, Abca7, Abcc12, Chtf18, Msh3, Plk4, Kdr, Orc1, Rfc4, Ears2
Nucleoside phosphate binding (GO:1901265)	22	2.56	1.45E-02	Ndor1, Irak3, Rab32, Enpp1, Sgk3, Mst1, Recql, Chek1, Lyn, Cdc7, Rasef, Pygl, Abca7, Abcc12, Chtf18, Msh3, Pold1, Plk4, Kdr, Orc1, Rfc4, Ears2
Nucleotide binding (GO:0000166)	22	2.56	1.33E-02	Ndor1, Irak3, Rab32, Enpp1, Sgk3, Mst1, Recql, Chek1, Lyn, Cdc7, Rasef, Pygl, Abca7, Abcc12, Chtf18, Msh3, Pold1, Plk4, Kdr, Orc1, Rfc4, Ears2
Small molecule binding (GO:0036094)	25	2.48	1.10E-02	Ndor1, Irak3, Rab32, Enpp1, Sgk3, Mst1, Recql, Chek1, Lyn, Cdc7, Rasef, Pygl, Abca7, Abcc12, Chtf18, Msh3, Pold1, Plk4, Rbp4, Kdr, Orc1, Comp, Rfc4, Ears2, Adap2
Anion binding (GO:0043168)	23	2.37	2.83E-02	Ndor1, Irak3, Rab32, Enpp1, Sgk3, Mst1, Recql, Chek1, Lyn, Cdc7, Rasef, Pygl, Abca7, Abcc12, Trpm2, Chtf18, Msh3, Plk4, Kdr, Orc1, Rfc4, Ears2, Adap2
Cation binding (GO:0043169)	34	2.21	5.60E-03	Pgm1, Irak3, Asah2, Galt, Enpp1, Adamts20, Zmynd10, Mst1, Tatdn3, Casz1, Lpl, Cdc7, Tert, Pygl, Pkd2, Dysf, Trpm2, Pold1, Mt2, Zbtb49, Mcm10, Galnt6, Csrp2, Thap1, Primpol, Orc1, Eya1, Comp, Pgm1, Ankmy1, Alox12, Ears2, Adap2, Fkbp7
Metal ion binding (GO:0046872)	33	2.21	6.80E-03	Pgm1, Irak3, Asah2, Galt, Enpp1, Adamts20, Zmynd10, Mst1, Tatdn3, Casz1, Lpl, Cdc7, Tert, Pkd2, Dysf, Trpm2, Pold1, Mt2, Zbtb49, Mcm10, Galnt6, Csrp2, Thap1, Primpol, Orc1, Eya1, Comp, Pgm1, Ankmy1, Alox12, Ears2, Adap2, Fkbp7
Ion binding (GO:0043167)	48	2.17	4.88E-05	Pgm1, Ndor1, Irak3, Asah2, Galt, Rab32, Enpp1, Adamts20, Zmynd10, Sgk3, Mst1, Recql, Tatdn3, Casz1, Chek1, Lyn, Lpl, Cdc7, Tert, Rasef, Pygl, Abca7, Abcc12, Pkd2, Dysf, Trpm2, Chtf18, Msh3, Pold1, Mt2, Zbtb49, Mcm10, Plk4, Galnt6, Csrp2, Thap1, Primpol, Kdr, Orc1, Eya1, Comp, Rfc4, Pgm1, Ankmy1, Alox12, Ears2, Adap2, Fkbp7
Catalytic activity (GO:0003824)	42	1.81	1.46E-02	Pgm1, Ndor1, Has1, Irak3, Asah2, Galt, Ddb2, Rab32, Enpp1, Adamts20, Sgk3, Mst1, Recql, Tatdn3, Pecr, Chek1, Lyn, Lpl, Cdc7, Tert, Rasef, Pygl, Casp7, Mettl23, Abca7, Abcc12, Trpm2, Mst1, Chtf18, Pold1

TABLE 7 (Continued)

Gene ontology annotation	# Genes	fold enrichment	False discovery rate	Genes
Binding (GO:0005488)	78	1.33	9.84E-03	Pgm1, Ptafr, Mks1, Rpl5, Ndor1, Has1, Irak3, Asah2, Galt, Ddb2, Nfatc4, Rab32, Nphp3, Enpp1, Adamts20, Itgbl1, Zmynd10, Pdgfb, Sgk3, Cort, Foxo4, Mst1, Recql, Tatdn3, Casz1, Pecr, Chek1, Lyn, Lpl, Coro6, Cdc7, Tert, Rasef, Pygl, Casp7, Reep6, Mettt123, Abca7, Sash3, Abcc12, Pkd2, Dysf, Trpm2, Psme2, Mst1, Chtf18, Msh3, Mphosph6, Hspb7, Hapln2, Pold1, Mt2, Zbtb49, Tbl2, Mcm10, Kcni4, Plk4, Bmper, Galnt6, Csrp2, Thap1, Klhl10, Primpol, Rbp4, Kdr, Orc1, Eya1, Comp, Rfc4, Pgm1, Ankmy1, Alox12, Ears2, Shroom1, Rabep2, Adap2, Npy, Fkbp7
Replication fork (GO:0005657)	5	17.84	2.55E-02	Chek1, Pold1, Mcm10, Primpol, Rfc4

higher maximum luminance when interacting with their partners than females did, and a strong correlation in maximum luminance with their partner during these changes. No females ever changed color while they were being used as a “stranger” stimulus animal.

Behavioral synchrony, as displayed by the seahorse pair mates by coordinating changes in luminance, is not absolutely necessary for a pair bond,⁶⁷ but is displayed by many pair bonding species^{68,69} and presumably reinforces the pair bond in species where it exists. We found some evidence of synchronous behavior, although these instances of synchronous color change numbered much fewer than instances when the male alone changed color. Moreover, the stronger ratio of luminance change that males performed when interacting with their partner compared to stranger females could also indicate that brightening the abdominal region could work as a visual signal to reinforce the pair bond. Similar flash displays are used by fish of different species to communicate with conspecifics or potential mates.⁷⁰ Many fishes, both freshwater and marine, have visual systems and color vision that may work differently from human vision.⁷⁰ As a result, to understand the behavioral tasks that vision enables including mate choice, feeding, agonistic behavior and camouflage, we need to see the world through a fish's eye. This form of social communication, and its symmetry or lack of symmetry between pair mates, may be useful as a measure of pair-bond quality.

Our initial study of gene expression changes that come with pairing in males produced suggestive results. Metabolic processes were implicated in more than one of our analyses; upregulation of these processes could be associated with social interest and neural activity related to pair-bond formation; with heightened locomotor activity because of the social engagement; with gearing up for male pregnancy; or with all the above. It is perhaps relevant that in multiple studies of pair-bond formation in male titi monkeys, whole brain glucose uptake was elevated.^{71,72}

Furthermore, there are intriguing indications that some of the neurochemical systems that have been associated with pair bonding in mammals are also involved in seahorses. We saw upregulation of the OT receptor gene in paired female seahorses, as well as upregulation of a serotonin receptor, Htr4, in paired male seahorses, when compared to the mean for all our subjects (i.e., when z-scored). Nonapeptides such as OT in mammals, MT in birds, reptiles, and amphibians, and IT in fish are known to be involved in the formation and maintenance of pair bonds (see Reference 6 for review). The relative increase in Oxt expression in paired female seahorses is qualitatively similar to the Oxt expression in paired male *Chaetodon lunulatus*, a butterfly fish that shows pair bonding behavior.¹³ Serotonin has also been implicated in the regulation of social behavior in mammals, although much less is known about its functions.^{73,74} However, this exploratory analysis was not corrected for multiple comparisons, and more work is necessary to determine what, if any, role these neurotransmitters play in social behaviors in seahorses.

Perhaps most interesting is the overlap in gene expression change induced by pairing in both male seahorses (this study) and the MPOA and NAcc of male prairie voles.⁶¹ The RRHO approach allows for an unbiased comparison between genes of interest that are found in

TABLE 8 Gene ontology annotations for downregulated genes identified through the comparisons of seahorse and vole NAcc using RRHO. The RRHO analysis identified genes that were downregulated in both the seahorse brain and prairie vole NAcc. We analyzed these genes for their associated gene ontology annotations. We identified annotations with a false discovery rate <0.05 as well as the specific genes linked to those annotations

Gene ontology annotation	# Genes	fold enrichment	False discovery rate	Genes
Sperm motility (GO:0097722)	6	12.81	3.00E-02	Spag6, Zmynd10, Nme8, Cfpap53, Spag6, Cfpap52
Cilium movement (GO:0003341)	7	10.55	4.48E-02	Spag6, Zmynd10, Nme8, Cfpap53, Dnah10, Spag6, Cfpap52
Ameboidal-type cell migration (GO:0001667)	7	10.12	3.89E-02	Spag6, Ret, Fgf2, Pkn2, Calca, Mixl1, Alx1
Movement of cell or subcellular component (GO:0006928)	18	3.37	7.26E-02	Spag6, Myot, Prtg, Zmynd10, Ret, Fgf2, Nme8, Cav3, Cfpap53, Pkn2, Agbl4, Dnah10, Calca, Mixl1, Spag6, Mypn, Alx1, Cfpap52
Multicellular organism development (GO:0007275)	35	2.03	3.18E-02	Spag6, Tyr, Myot, Rhag, Trpv1, Prtg, Fgl1, Ret, Epor, Mfrp, Fgf2, Pparg, Jun, Angptl3, Nme8, Cav3, Esp1, Cfpap53, Edar, Agbl4, Plk4, Serpine1, Esco2, Nrl, Calca, Tbeta, Mixl1, Spag6, Mypn, Alx1, Cfpap52, Itpkb, Cited1, Myl7, C6
Axoneme (GO:0005930)	6	12.17	2.55E-02	Spag6, Nme8, Cfpap53, Dnah10, Spag6, Cfpap52
Ciliary plasm (GO:0097014)	6	12	1.38E-02	Spag6, Nme8, Cfpap53, Dnah10, Spag6, Cfpap52
Plasma membrane bounded cell projection cytoplasm (GO:0032838)	6	9.19	2.92E-02	Spag6, Nme8, Cfpap53, Dnah10, Spag6, Cfpap52
Cytoplasmic region (GO:0099568)	7	8.73	1.26E-02	Spag6, Gck, Nme8, Cfpap53, Dnah10, Spag6, Cfpap52

different regions and/or species.^{16,63,64} The RRHO analysis identifies differentially expressed genes in a sample, ranks them in a list according to their log-fold change, and compares that ranked list to lists from another dataset with a similar experimental manipulation.

Traditional quantitative RNAseq analyses directly compare the expression of specific genes between groups, and the regions of interest are closely matched to minimize variability and maximize “signal” relative to “noise.” The RRHO analysis allows us to directly compare gene expression between unmatched regions of interest because the “signal” (i.e., the genes of interest) are not removed through a thresholding process. Thus, whole brain RNAseq will generate a broad list of differentially expressed genes, and the “signal” from the region of interest would be present, albeit reduced because of the additional irrelevant information. The list of genes from smaller regions of interest should have a stronger “signal” as a result of the decreased variability of the tissue. The genes on the whole brain list that are not on the region of interest list should just drop out of the analysis, thus eliminating many irrelevant genes. The genes on the whole brain list that have strong signal, despite the dilution of the broader area, will still show up in the ranked list and be picked up by the analysis. In this experiment, the relative strength of signal is illustrated by the difference in the magnitude of *p*-values between the MPOA/NAcc comparison and the comparisons between the whole seahorse brain and vole brain regions. The higher *p*-value in the whole-brain comparisons (seahorse vs. vole NAcc and seahorse vs. vole MPOA) reflects the extraneous genes found in the whole brain that did not correspond to genes in the smaller region of interest.

Here we compared gene expression found in the whole brains of seahorses against gene expression in the MPOA and NAcc of prairie voles. The MPOA and NAcc are known to play important roles in establishing and maintaining pair bonds,^{71,75,76} so it is not surprising to find large amounts of significant overlap between genes expressed in these regions. Genes up-regulated similarly in both seahorses and the MPOA of voles include components of hormone systems regulating reproduction including progesterone, estrogen and androgens; as well as luteinizing hormone and corticotropin releasing hormone (Supplementary Table 1). The predominance of the reproductive pathways may reflect that the MPOA is a key area for male sexual behavior and reproduction in mammals.^{61,77} Additional comparisons, with more areas from vole brains and more specificity in seahorse brain, will be useful in disentangling these results.

Another commonality between seahorses and voles is the upregulation (and downregulation) in genes associated with cilia; ciliary organization genes were also implicated in the GO analysis. Cilia, which are present on both neurons and glial cells, receive diverse types of information and modulate cellular function.⁷⁸ Neural plasticity has been studied in association with parenting,^{79,80} and with sexual experience,⁸¹ and it is likely that it is important in the formation of pair bonds as well. Cilia are less well studied in the context of adult neural plasticity,⁸² making this an exciting area to pursue in the neurobiology of social behavior.

There were a number of limitations that may have affected our results. First, our sample size of 10 seahorses (three pairs and four

unpaired males) requires replication of many of our findings, although the current study establishes a foundation for future research. While the sample size was similar to the number used in other genomic studies,^{16,83,84} the use of an outbred species and the whole brain likely increased variability in results. This small sample size, and large amount of variation, is also the reason that we did not present preference behavior from the PPT in the current manuscript; a larger sample size will be necessary to fully explore that variation. We also had limited information about the seahorses we received from the vendor. Their age, reproductive status and prior experience could have had effects on the behavior and genomic data we acquired. For example, in cichlid fish, evidence has shown that reproductive state has an effect on female preference,⁸⁵ and in prairie voles, prior pair-bonding experience had an effect on the ability to re-bond and the strength of the new bond.⁸⁶ We did attempt to create commonality of recent experience by housing all animals in same-sex herds for 4 months before pairing; however, these demographic factors could have influenced behavior including luminance synchrony.

The main challenge in our gene expression analyses was the small size of the brain. We opted for extraction of RNA from whole brain because of this small size, overall low-cellular density, and our desire to obtain individual rather than pooled data. For future experiments, we have explored the idea of utilizing an emerging method of spatial transcriptomics to get spatial data from brains of such small size to better understand gene expression throughout the brain at a single cell level.⁸⁷ There is also the question of how meaningful the gene expression data is when comparing paired and unpaired seahorses, given the variability of the behaviors exhibited by the subjects. Variability is a characteristic of pair bonds in many species,⁶⁷ including both prairie voles⁸⁸ and humans.⁸⁹ This is certainly a valid concern, and we view the gene expression analysis as a starting point that will inform future studies. At a minimum, the gene expression data here have showed that similar patterns of differential gene expression are found within the brains of paired male seahorses and prairie voles, which suggests that similar neural and neuroendocrine systems are involved across both species.

Future research will examine the pair bond behaviors of seahorses and manipulate conditions that may affect these pair bonds (e.g., stocking density and sex ratios).⁹⁰ Future studies will expand upon these findings, including further validation of the PPT as well as exploration of the time course of preference formation in this species. We plan to investigate the neuroendocrine and genetic basis of these behaviors, as well as the function of particular behaviors, reproductive success, and other characteristics of the pair bond such as mate guarding and stress buffering, and compare them to behaviors seen in socially monogamous mammals. As such, seahorses may also be valuable as a new biomedical research animal, in the same way that prairie voles have enriched our universe of biomedical rodent models. Ultimately this research will illuminate the evolutionary history and mechanisms of these complex social behaviors.

ACKNOWLEDGMENTS

Colby Johnson reports part-ownership of Aquabiomics, Inc. The other authors report no conflicts of interest. This research was funded by

the Good Nature Institute, as well as the College of Biological Sciences and Department of Neurobiology, Physiology, and Behavior at the University of California, Davis. We would like to thank the animal care staff at the UC-Davis Teaching and Research Animal Care Facility for their exceptional care of these subjects, Jessica Bond for research support, and Brian Trainor for helpful analytical suggestions. Rafael C. Duarte is supported by Fundação de Amparo à Pesquisa do Estado de São Paulo through a post-doctoral fellowship (FAPESP: #2019/01934-3). The sequencing was carried by the DNA Technologies and Expression Analysis Core at the UC Davis Genome Center, supported by NIH Shared Instrumentation Grant 1S10OD010786-01.

DATA AVAILABILITY STATEMENT

The genomic data that support this study are openly available at NCBI's sequence read archive (<https://www.ncbi.nlm.nih.gov/>) under accession numbers SAMN20710037 to SAMN20710056. The behavioral data that support this study are included in Supplementary Table 5.

ORCID

Karen L. Bales  <https://orcid.org/0000-0001-5826-2095>

REFERENCES

- Gillette JR, Jaeger RG, Peterson MG. Social monogamy in a territorial salamander. *Anim Behav.* 2000;59(6):1241-1250. doi:10.1006/anbe.2000.1437
- French JA, Cavanaugh J, Mustoe AC, Carp SB, Womack SL. Social monogamy in nonhuman primates: phylogeny, phenotype, and physiology. *J Sex Res.* 2018;55(4-5):410-434. doi:10.1080/00224499.2017.1339774
- Kleiman DG. Monogamy in mammals. *Q Rev Biol.* 1977;52:39-69.
- Lukas D, Clutton-Brock TH. The evolution of social monogamy in mammals. *Science.* 2013;341:526-530.
- Whiteman EA, Côté IM. Monogamy in marine fishes. *Biol Rev.* 2004;79(2):351-375. doi:10.1017/S1464793103006304
- Fischer EK, Nowicki JP, O'Connell LA. Evolution of affiliation: patterns of convergence from genomes to behaviour. *Philos Trans Royal Soc B: Biol Sci.* 2019;374(1777):20180242. doi:10.1098/rstb.2018.0242
- Hazan C, Shaver P. Romantic love conceptualized as an attachment process. *J Pers Soc Psychol.* 1987;52(3):511-524.
- Mason WA, Mendoza SP. Generic aspects of primate attachments: parents, offspring and mates. *Psychoneuroendocrinology.* 1998;23(8):765-778.
- O'Connor CM, Marsh-Rollo SE, Aubin-Horth N, Balshine S. Species-specific patterns of nonapeptide brain gene expression relative to pair-bonding behavior in grouping and non-grouping cichlids. *Horm Behav.* 2016;80:30-38. doi:10.1016/j.yhbeh.2015.10.015
- Oldfield RG, Hofmann HA. Neuropeptide regulation of social behavior in a monogamous cichlid fish. *Physiol Behav.* 2011;102(3-4):296-303. doi:10.1016/j.physbeh.2010.11.022
- Garrison JL, Macosko EZ, Bernstein S, Pokala N, Albrecht DR, Bargmann CI. Oxytocin/vasopressin-related peptides have an ancient role in reproductive behavior. *Science.* 2012;338:540-543.
- Dewan AK, Ramey ML, Tricas TC. Arginine vasotocin neuronal phenotypes, telencephalic fiber varicosities, and social behavior in butterflyfishes (Chaetodontidae): potential similarities to birds and mammals. *Horm Behav.* 2011;59(1):56-66. doi:10.1016/j.yhbeh.2010.10.002
- Nowicki JP, Pratchett MS, Walker SPW, Coker DJ, O'Connell LA. Gene expression correlates of social evolution in coral reef butterflyfishes. *Proc Royal Soc London Series B: Biol Sci.* 2020;207:7.

14. Lim MM, Wang Z, Olazabal DE, Ren X, Terwilliger EF, Young LJ. Enhanced partner preference in a promiscuous species by manipulating the expression of a single gene. *Nature*. 2004;429(6993):754-757.
15. Nair HP, Young LJ. Vasopressin and pair-bond formation: genes to brain to behavior. *Phys Ther*. 2006;21(2):146-152. doi:10.1152/physiol.00049.2005
16. Young RL, Ferkin MH, Ockendon-Powell NF, et al. Conserved transcriptomic profiles underpin monogamy across vertebrates. *Proc Natl Acad Sci U S A*. 2019;116(4):1331-1336. doi:10.1073/pnas.1813775116
17. Renn SCP, Machado HE, Duftner N, Sessa AK, Harris RM, Hofmann HA. Gene expression signatures of mating system evolution. *Genome*. 2018;61(4):287-297. doi:10.1139/gen-2017-0075
18. Vincent ACJ, Sadler LM. Faithful pair bonds in wild seahorses. *Hippocampus Whitei Animal Behav*. 1995;50(6):1557-1569. doi:10.1016/0003-3472(95)80011-5
19. Masonjones H, Lewis S. Courtship behavior in the dwarf seahorse, *Hippocampus zosterae*. *Am Soc Ichthyol Herpetol*. 1996;3:634-640. doi:10.2307/1447527
20. Jones AG, Kvarnemo C, Moore GI, Simmons LW, Avise JC. Microsatellite evidence for monogamy and sex-biased recombination in the Western Australian seahorse *Hippocampus angustus*. *Mol Ecol*. 1998;7(11):1497-1505. doi:10.1046/j.1365-294x.1998.00481.x
21. Grange N, Cretchley R. A preliminary investigation of the reproductive behaviour of the Knysna seahorse, *Hippocampus capensis* Boulenger, 1900. *Southern African J Aquatic Sci*. 1995;21(1-2):103-104. doi:10.1080/10183469.1995.9631367
22. Kvarnemo C, Moore GI, Jones AG, Nelson WS, Avise JC. Monogamous pair bonds and mate switching in the Western Australian seahorse *Hippocampus subelongatus*. *J Evol Biol*. 2000;13(6):882-888. doi:10.1046/j.1420-9101.2000.00228.x
23. Wilson AB, Martin-Smith KM. Genetic monogamy despite social promiscuity in the pot-bellied seahorse (*Hippocampus abdominalis*). *Mol Ecol*. 2007;16(11):2345-2352. doi:10.1111/j.1365-294X.2007.03243.x
24. Lin T, Liu X, Zhang D, Li S. Female lined seahorses (*Hippocampus erectus*) recognize their mates based on olfactory cues. *Behav Processes*. 2021;189:104419. doi:10.1016/j.beproc.2021.104419
25. Lin T, Liu X, Zhang D. Does the female seahorse still prefer her mating partner after a period of separation? *J Fish Biol*. 2021;99(5):1613-1621. doi:10.1111/jfb.14867
26. Williams JR, Slotnick BM, Kirkpatrick BW, Carter CS. Olfactory bulb removal affects partner preference development and estrus induction in female prairie voles. *Physiol Behav*. 1992;52:635-639.
27. DeVries AC, Carter CS. Sex differences in temporal parameters of partner preference in prairie voles (*Microtus ochrogaster*). *Can J Zool-Revue Canadienne de Zool*. 1999;77(6):885-889.
28. Millan MJ, Bales KL. Towards improved animal models for evaluating social cognition and its disruption in schizophrenia: the CNTRICS initiative. *Neurosci Biobehav Rev*. 2013;37(9):2166-2180. doi:10.1016/j.neubiorev.2013.09.012
29. Freret-Meurer NV, Andreatta JV, Alves MAS. Activity rate of the seahorse *Hippocampus reidi* Ginsburg, 1933 (Syngnathidae). *Acta Ethol*. 2012;15(2):221-227. doi:10.1007/s10211-012-0125-1
30. Woodall LC, Koldewey HJ, Santos SV, Shaw PW. First occurrence of the lined seahorse *Hippocampus erectus* in the eastern Atlantic Ocean. *J Fish Biol*. 2009;75(6):1505-1512. doi:10.1111/j.1095-8649.2009.02371.x
31. Lourie SA, Randall JE. A new pygmy seahorse, *Hippocampus denise* (Teleostei: Syngnathidae), from the Indo-Pacific. *Zool Studies*. 2003;42(2):284-291.
32. Beeching SC. Colour pattern and inhibition of aggression in the cichlid fish *Astronotus ocellatus*. *J Fish Biol*. 1995;47(1):50-58. doi:10.1111/j.1095-8649.1995.tb01872.x
33. Carter SC, DeVries CA, Getz LL. Physiological substrates of mammalian monogamy: the prairie vole model. *Neurosci Biobehav Rev*. 1995;19(2):303-314. doi:10.1016/0149-7634(94)00070-H
34. Walum H, Young LJ. The neural mechanisms and circuitry of the pair bond. *Nat Rev Neurosci*. 2018;19(11):643-654. doi:10.1038/s41583-018-0072-6
35. Williams JR, Insel TR, Harbaugh CR, Carter CS. Oxytocin administered centrally facilitates formation of a partner preference in female prairie voles (*Microtus ochrogaster*). *J Neuroendocrinol*. 1994;6(3):247-250. doi:10.1111/j.1365-2826.1994.tb00579.x
36. Carp SB, Rothwell ES, Bourdon A, Freeman SM, Ferrer E, Bales KL. Development of a partner preference test that differentiates between established pair bonds and other relationships in socially monogamous titi monkeys (*Callicebus cupreus*). *Am J Primatol*. 2016;78(3):326-339. doi:10.1002/ajp.22450
37. Roselli CE, Stormshak F. The neurobiology of sexual partner preferences in rams. *Horm Behav*. 2009;55(5):611-620. doi:10.1016/j.yhbeh.2009.03.013
38. Leese JM. Sex differences in the function of pair bonding in the monogamous convict cichlid. *Anim Behav*. 2012;83(5):1187-1193. doi:10.1016/j.anbehav.2012.02.009
39. Walling CA, Royle NJ, Lindström J, Metcalfe NB. Do female association preferences predict the likelihood of reproduction? *Behav Ecol Sociobiol*. 2010;64(4):541-548. doi:10.1007/s00265-009-0869-4
40. Gonçalves DM, Oliveira RF. Time spent close to a sexual partner as a measure of female mate preference in a sex-role-reversed population of the blenny *Salarias pavo* (Risso) (Pisces: Blenniidae). *Acta Ethol*. 2003;6(1):1-5. doi:10.1007/s10211-003-0083-8
41. Alexander G, Couldridge V. Does the time spent near a male predict female mate choice in a Malawian cichlid? *J Fish Biol*. 2001;59:667-672.
42. van den Berg CP, Troscianko J, Endler JA, Marshall NJ, Cheney KL. Quantitative colour pattern analysis (QCPA): a comprehensive framework for the analysis of colour patterns in nature. *Methods Ecol Evol*. 2020;11(2):316-332. doi:10.1111/2041-210X.13328
43. Stevens M, Párraga AC, Cuthill IC, Partridge JC, Troscianko TS. Using digital photography to study animal coloration. *Biol J Linn Soc*. 2007;90(2):211-237. doi:10.1111/j.1095-8312.2007.00725.x
44. Troscianko J, Stevens M. Image calibration and analysis toolbox – a free software suite for objectively measuring reflectance, colour and pattern. *Methods Ecol Evol*. 2015;6(11):1320-1331. doi:10.1111/2041-210X.12439
45. Mosk V, Thomas N, Hart NS, Partridge JC, Beazley LD, Shand J. Spectral sensitivities of the seahorses *Hippocampus subelongatus* and *Hippocampus barbouri* and the pipefish *Stigmatopora argus*. *Vis Neurosci*. 2007;24(3):345-354. doi:10.1017/S0952523807070320
46. Duarte RC, Stevens M, Flores AAV. The adaptive value of camouflage and colour change in a polymorphic prawn. *Sci Rep*. 2018;8(1):16028. doi:10.1038/s41598-018-34470-z
47. Dias TL, Rosa IL, Baum JK. Threatened fishes of the world: *Hippocampus erectus* Perry, 1810 (Syngnathidae). *Environ Biol Fishes*. 2002;65(3):326. doi:10.1023/A:1020539222587
48. Wyszecki G, Stiles WS. *Color Science: Concepts and Methods, Quantitative Data and Formulae*. 2nd ed. John Wiley & Sons; 2000.
49. Bakdash JZ, Marusich LR. Repeated measures correlation. *Front Psychol*. 2017;8:456. doi:10.3389/fpsyg.2017.00456
50. Lourie SA. Measuring Seahorses. 2003. https://static1.squarespace.com/static/55930a68e4b08369d02136a7/t/5639576ce4b05b184b56cb40/1446598508315/Measuring_Seahorses.pdf
51. Dobin A, Davis CA, Schlesinger F, et al. STAR: ultrafast universal RNA-seq aligner. *Bioinformatics*. 2013;29(1):15-21. doi:10.1093/bioinformatics/bts635
52. Lin Q, Fan S, Zhang Y, et al. The seahorse genome and the evolution of its specialized morphology. *Nature*. 2016;540(7633):395-399. doi:10.1038/nature20595
53. R Studio Team. RStudio: Integrated Development for R. <http://www.rstudio.com>

54. Ritchie ME, Phip B, Wu D, et al. limma powers differential expression analyses for RNA-sequencing and microarray studies. *Nucleic Acids Res.* 2021;43:e47. <https://academic.oup.com/nar/article/43/7/e47/2414268?login=true>
55. Law CW, Chen Y, Shi W, Smyth GK. Voom: precision weights unlock linear model analysis tools for RNA-seq read counts. *Genome Biol.* 2014;15(2):R29. doi:10.1186/gb-2014-15-2-r29
56. Benjamini Y, Hochberg Y. Controlling the false discovery rate: a practical and powerful approach to multiple testing. *J R Stat Soc Series B Stat Methodology.* 1995;57:289-300.
57. Kolmogorov-Smirnov Test. *The Concise Encyclopedia of Statistics.* Springer; 2008:283-287. doi:10.1007/978-0-387-32833-1_214
58. Alexa A, Rahnenfuhrer J. TopGO: Enrichment analysis for gene ontology. Bioconductor version: Release (3.13); 2021. doi:10.18129/B9.bioc.topGO
59. Wilcoxon HW. Rank Sum Test. In: Dubitzky W, Wolkenhauer O, Cho KH, Yokota H, eds. *Encyclopedia of Systems Biology.* Springer; 2013:2354-2355. doi:10.1007/978-1-4419-9863-7_1185
60. Tenenbaum D, Volkening J, Maintainer BP. KEGGREST: Client-side rest access to the Kyoto encyclopedia of genes and genomes (KEGG). Bioconductor Version: Release (3.13); 2021. doi:10.18129/B9.bioc.KEGGREST
61. Seelke AMH, Bond JM, Simmons TC, et al. Fatherhood alters gene expression within the MPOA. *Environ Epigenet.* 2018;4(4):1-17. doi:10.1093/eep/dvy026
62. Duclot F, Sailer L, Koutakis P, Wang Z, Kabbaj M. Transcriptomic regulations underlying pair-bond formation and maintenance in the socially monogamous male and female prairie vole. *Biol Psychiatr.* 2020;9:141-151. doi:10.1016/j.biopsych.2020.11.022
63. Cahill KM, Huo Z, Tseng GC, Logan RW, Seney ML. Improved identification of concordant and discordant gene expression signatures using an updated rank-rank hypergeometric overlap approach. *Sci Rep.* 2018;8(1):9588. doi:10.1038/s41598-018-27903-2
64. Plaisier SB, Taschereau R, Wong JA, Graeber TG. Rank-rank hypergeometric overlap: identification of statistically significant overlap between gene-expression signatures. *Nucleic Acids Res.* 2010;38(17):e169. doi:10.1093/nar/gkq636
65. Rosenblatt JD, Stein JL. RRHO: Test overlap using the rank-rank hypergeometric test; 2014.
66. Li C, Olave M, Hou Y, et al. Genome sequences reveal global dispersal routes and suggest convergent genetic adaptations in seahorse evolution. *Nat Commun.* 2021;12(1):1094. doi:10.1038/s41467-021-21379-x
67. Bales KL, Ardekani CS, Baxter A, et al. What is a pair bond? *Horm Behav.* 2021;136:105062.
68. Menzel CR. Coordination and conflict in *Callicebus* social groups. In: Mason WA, Mendoza SP, eds. *Primate Social Conflict.* State University of New York Press; 1993:253-290.
69. Dunbar RIM, Dunbar EP. The pairbond in klipspringer. *Anim Behav.* 1980;28:219-229.
70. Marshall NJ, Cortesi F, de Busserolles F, Siebeck UE, Cheney KL. Colours and colour vision in reef fishes: past, present and future research directions. *J Fish Biol.* 2019;95(1):5-38. doi:10.1111/jfb.13849
71. Bales KL, Mason WA, Catana C, Cherry SR, Mendoza SP. Neural correlates of pair-bonding in a monogamous primate. *Brain Res.* 2007;1184(1):245-253. doi:10.1016/j.brainres.2007.09.087
72. Maninger N, Hinde K, Mendoza SP, et al. Pair bond formation leads to a sustained increase in global cerebral glucose metabolism in monogamous male titi monkeys (*Callicebus cupreus*). *Neuroscience.* 2017;348:302-312. doi:10.1016/j.neuroscience.2017.02.028
73. Larke R, Maninger N, Ragen B, Mendoza SP, Bales KL. Serotonin 1A agonism decreases affiliative behavior in pair-bonded titi monkeys. *Horm Behav.* 2016;86:71-77. doi:10.1016/j.yhbeh.2016.10.001
74. Dölen G, Darvishzadeh A, Huang KW, Malenka RC. Social reward requires coordinated activity of accumbens oxytocin and 5HT. *Nature.* 2013;501(7466):179-184. doi:10.1038/nature12518
75. Shahrokh DK, Zhang TY, Diorio J, Gratton A, Meaney MJ. Oxytocin-dopamine interactions mediate variations in maternal behavior in the rat. *Endocrinology.* 2010;151(5):2276-2286. doi:10.1210/en.2009-1271
76. Aragona BJ, Wang Z. The prairie vole (*Microtus ochrogaster*): an animal model for behavioral neuroendocrine research on pair bonding. *ILAR J.* 2004;45(1):35-45. doi:10.1093/ilar.45.1.35
77. Hull EM, Dominguez JM. Sexual behavior in male rodents. *Horm Behav.* 2007;52:45-55.
78. Liu S, Trupiano M, Simon J, Guo J, Anton ES. The essential role of primary cilia in cerebral cortical development and disorders. *Current Topics in Developmental Biology.* Vol 142. Academic Press; 2021. doi:10.1016/bs.ctdb.2020.11.003
79. Leuner B, Glasper ER, Gould E. Parenting and plasticity. *Trends Neurosci.* 2010;33(10):465-473. doi:10.1016/j.tins.2010.07.003
80. Glasper ER, Schoenfeld TJ, Gould E. Adult neurogenesis: optimizing hippocampal function to suit the environment. *Behav Brain Res.* 2012;227(2):380-383. doi:10.1016/j.bbr.2011.05.013
81. Glasper ER, Gould E. Sexual experience restores age-related decline in adult neurogenesis and hippocampal function. *Hippocampus.* 2013;23(4):303-312. doi:10.1002/hipo.22090
82. Kirschen GW, Xiong Q. Primary cilia as a novel horizon between neuron and environment. *Neural Regen Res.* 2017;12(8):1225-1230. doi:10.4103/1673-5374.213535
83. Das B, de Bekker C. Time-course RNASeq of *Camponotus floridanus* forager and nurse ant brains indicate links between plasticity in the biological clock and behavioral division of labor. *BMC Genomics.* 2022;23(1):57. doi:10.1186/s12864-021-08282-x
84. Steffen MA, Rehan SM. Genetic signatures of dominance hierarchies reveal conserved cis-regulatory and brain gene expression underlying aggression in a facultatively social bee. *Genes Brain Behav.* 2020;19(1):e12597. doi:10.1111/gbb.12597
85. Clement TS, Grens KE, Fernald RD. Female affiliative preference depends on reproductive state in the African cichlid fish. *Astatotilapia Burtoni Behav Ecol.* 2005;16(1):83-88. doi:10.1093/beheco/arl134
86. Harbert KJ, Pellegrini M, Gordon KM, Donaldson ZR. How prior pair-bonding experience affects future bonding behavior in monogamous prairie voles. *Horm Behav.* 2020;126:104847. doi:10.1016/j.yhbeh.2020.104847
87. Lein E, Borm LE, Linnarsson S. The promise of spatial transcriptomics for neuroscience in the era of molecular cell typing. *Science.* 2017;358(6359):64-69. doi:10.1126/science.aan6827
88. Vogel AR, Patisaul HB, Arambula SE, Tiezzi F, McGraw LA. Individual variation in social behaviours of male lab-reared prairie voles (*Microtus ochrogaster*) is non-heritable and weakly associated with V1aR density. *Sci Rep.* 2018;8:1396.
89. Quinlan RJ. Human pair-bonds: evolutionary functions, ecological variation, and adaptive development. *Evol Anthropol.* 2008;17:227-238. doi:10.1002/evan.20191
90. Mobley KB, Jones AG. Geographical variation in the mating system of the dusky pipefish (*Syngnathus floridae*). *Mol Ecol.* 2007;16(12):2596-2606. doi:10.1111/j.1365-294X.2007.03337.x

SUPPORTING INFORMATION

Additional supporting information may be found in the online version of the article at the publisher's website.

How to cite this article: Mederos SL, Duarte RC, Mastoras M, et al. Effects of pairing on color change and central gene expression in lined seahorses. *Genes, Brain and Behavior.* 2022; 21(5):e12812. doi:10.1111/gbb.12812